February 6, 2023 Türkiye Earthquakes:

GEER Phase 3 Team Report on Selected Geotechnical Engineering Effects

By

Diane Moug, Patrick Bassal, Jonathan D. Bray, K. Önder Çetin, Sena Begüm Kendir, Arda Şahin, Elife Çakır, Berkan Söylemez, and Soner Ocak

A report prepared by the Geotechnical Extreme Event Reconnaissance Association (USA), Middle East Technical University (Türkiye), and Zemin Etüd ve Tasarım A.Ş. (Türkiye).

GEER Association Report 082-S1

https://doi.org/10.18118/G6F379

June 30, 2023

EXECUTIVE SUMMARY

This report presents the GEER Phase 3 team reconnaissance efforts following the February 6, 2023 Kahramanmaraş earthquake sequence. Reconnaissance was performed from March 27 to April 1, 2023 in and around İskenderun, Hatay; Gölbaşı, Adıyaman; and Antakya, Hatay. The objectives of the GEER Phase 3 team were to build upon the work of the previous GEER teams and partners by gathering detailed data to develop well documented field case histories in high priority areas. The reconnaissance efforts focused on surveying liquefaction effects including building settlement, lateral spreading, and flooding in Iskenderun and Gölbaşı, documenting bridge performance in and near Antakya, and observing fill settlement at a hospital near Antakya.

Evidence of extensive liquefaction was documented in Iskenderun and Gölbaşı. Large amounts of ejecta with significant building settlement and lateral spreading occurred in İskenderun. Additionally, regular flooding now takes place in coastal areas of İskenderun since the February 6 earthquakes due to land subsidence. The liquefaction effects of ejecta, building settlement, and lateral spreading were observed in Gölbaşı. Sampled ejecta from surveyed areas in Gölbaşı have plasticity indices of 9 to 14 or 16 to 23, as reported by Zemin Etüd ve Tasar Tasarım m A.Ş. (ZETAŞ) and Middle East Technical University (METU) laboratories, respectively.

The settlement at 22 buildings was surveyed in İskenderun, including 4 groups of buildings where interactions between the buildings and ground were documented. Building settlements between 0 cm to over 70 cm were documented in İskenderun. Liquefaction and building settlement were concentrated in the Çay district; however, building settlement was also documented in other waterfront areas of İskenderun. Building interactions included hogging and sagging ground deformations. In one case, at a restaurant called Pallet Hookah, the hogging ground deformation from the settlement of two adjacent buildings, appeared to have caused extensional damage to the structure slab and façade.

The settlement at 12 buildings was surveyed in Gölbaşı. The surveyed settlements ranged from 0 cm to over 100 cm. In two documented cases, adjacent and similar buildings in the same apartment complexes had markedly different performance; the difference between these buildings was that one had a basement and the other did not.

Lateral spreading ground failure with lateral displacements up to 150 cm was documented near the İskenderun shoreline. Lateral spread transects were measured to document differences between free field lateral spreads and lateral spreads in developed areas and between buildings.

Four bridges were documented in detail in Antakya. Damage at the bridges included observations of bridge deck movement and strains relative to the abutments and piers, tilting and pile damage at the abutments, and slope failures near the abutments. In one case, failure of the retaining walls near the bridge abutments was observed.

Severe compacted earth fill settlement was documented at a hospital near Antakya. The hospital was not in use following the earthquake. Fill settlement of up to 50 cm affected many of the hospital entrances.

TABLE OF CONTENTS

1.INTRODUCTION AND SCOPE OF RECONNAISSANCE

1.1 Event Overview

The first earthquake of the Kahramanmaraş earthquake sequence struck on February 6, 2023 at around 4:15 am local time. It was a moment magnitude (M_w) 7.8 event on the East Anatolian Fault. A M_w 6.7 aftershock occurred 11 minutes after it, which was followed by a M_w 7.5 earthquake 9 hours after the first earthquake (USGS 2023). Slightly higher M_w values have been estimated by some researchers (e.g., Okuwaki et al. 2023). Additionally, a M_w 6.3 aftershock on February 20 affected the Hatay Province region. These earthquakes caused widespread damage in Türkiye and Syria. The Kahramanmaraş earthquake sequence and the resulting infrastructure damage was extensive. At the time of this report, over 50,000 people lost their lives in Türkiye. There was widespread building collapse, with up to 80% of buildings collapsed in some areas. It is estimated that over 13.4 million people were impacted by this earthquake sequence.

1.2 Scope of Reconnaissance

The Geotechnical Extreme Events Reconnaissance (GEER) organization, in partnership with researchers at the Middle Eastern Technical University (METU) and Earthquake Engineering Research Institute (EERI) mobilized reconnaissance teams to learn from the Kahramanmaraş earthquakes. The initial response team was deployed in mid-February 2023 with the objective of collecting an overview of observations that would guide the Phase 2 reconnaissance efforts. The Phase 2 team was deployed in late February through early March 2023; the Phase 2 team's observations included ejecta, lateral spreading, building settlements, and inspection of seismic monitoring stations. Reconnaissance efforts were also coordinated with the EERI's Learning from Earthquakes (LFE) teams. The scope of the EERI LFE reconnaissance included lifelines, bridges, buildings, and hospitals.

This report presents the observations and surveys of the GEER Phase 3 team. The objective of this team was to build on the efforts of the first two GEER teams by concentrating data collection efforts at informative field case history sites. The team was led by Dr. Jonathan Bray (University of California, Berkeley), and its members included Dr. Patrick Bassal (The Ohio State University), Sena Begüm Kendir (Zemin Etüd ve Tasarim A.Ş.), and Dr. Diane Moug (Portland State University). The GEER Phase 3 team also collaborated in the field with researchers from Middle Eastern Technical Univeristy (METU): Dr. K. Önder Çetin, Arda Şahin, Elife Çakir, Berkan Söylemez, and Sonar Ocak.

The GEER Phase 3 team's reconnaissance activities were performed from March 27 until April 1, 2023. March 27, 28, 29 and April 1 were spent in İskenderun, Hatay Province, where reconnaissance efforts focused on surveying liquefaction effects including building settlement,

lateral spreading, and other ground deformations. March 30 was spent in Gölbaşı, Adıyaman Province, where reconnaissance efforts, in collaboration with Dr. K. Önder Çetin and his graduate students at METU, focused on surveying liquefaction effects on buildings and collecting soil ejecta samples. March 31 was spent in and nearby Antakya, Hatay Province, to investigate evidence of liquefaction and ground failure, and to survey selected bridges affected by ground deformations.

1.3 Previous 2023 Kahramanmaraş Earthquakes GEER Report

A joint GEER-EERI report on the 2023 Kahramanmaraş Earthquakes was published on May 6, 2023 (GEER-EERI 2023). That report summarizes reconnaissance efforts conducted by the Phase 1 and 2 GEER teams and the Buildings and Lifelines EERI teams, with preliminary observations of the GEER Phase 3 team. This GEER Phase 3 team report is intended to supplement the preliminary GEER-EERI report by providing a comprehensive documentation of the detailed surveys conducted by the GEER Phase 3 team.

1.4 Report Organization

Following this introduction section, liquefaction and ground failure observations are summarized in Section 2. The observations come from İskenderun, Hatay; Golbaşi, Adıyaman, and Antakya, Hatay. In İskenderun, widespread ground failure from liquefaction and lateral spreading was observed. Liquefaction and lateral spreading in İskenderun appear to primarily have occurred in the reclaimed, shorefront areas. Lateral spreading along seven transects was measured, with accumulated displacements measured to be as high as 150 cm. Extensive flooding was also observed in coastal areas of İskenderun, likely due to widespread ground settlement among other factors. In Gölbaşı, notable liquefaction was also observed, including many instances of liquefaction ejecta remaining from the earthquake events. Measured plasticity indices on the sampled ejecta ranged from 9 to 14. The Phase 3 team did not observe evidence of liquefaction in Antakya, Hatay; however, previous reconnaissance teams and remote sensing studies indicated liquefaction near Antakya, including lateral spreading along the Orontes river, and ejecta at the Hatay airport. Significant fill settlement was observed at a major hospital in Hatay Province.

Building settlement, tilting, and interactions between buildings and the ground are summarized in Section 3. Efforts focused on detailed surveys involving several hand and laser-level measurements, which were often accompanied with terrestrial lidar scans (FARO Focus3D X 330 2014). A total of 22 buildings were surveyed in İskenderun with settlements ranging from negligible to over 70 cm. Hogging or sagging ground deformations due to building settlements were documented for four groups of neighboring buildings. Twelve buildings were surveyed in Gölbaşı with settlements ranging from negligible to over 1 m. In two cases, two apartment buildings in the same complex and of similar design and age, except for one building having a basement and the other not having a basement, performed notably different.

Observations of the performance of transportation infrastructure are summarized in Section 4. These observations are primarily limited to bridges in the Hatay Province around Antakya. The observations include damage to structural components, compression and extension of the bridge deck relative to the approaches, damage to abutments, and retaining wall and slope failures near the abutments. Also included are observations of a U-box underpass in İskenderun where flooding was observed soon after the earthquake.

2. LIQUEFACTION AND GROUND FAILURE

2.1 Liquefaction

2.1.1 İskenderun, Hatay

Documented liquefaction-induced sediment ejecta and ground deformations were widespread in the shorefront area of İskenderun, particularly in the Çay district. The map in Figure 2.1 shows where the GEER Phase 2 team observed liquefaction ejecta. Additionally, previous reconnaissance teams observed ejecta at the İskenderun Port, which is not documented in Figure 2.1. Sediment ejecta were not sampled for characterization by the GEER Phase 3 team because previous GEER and METU teams had collected samples soon after the earthquake. Additionally, the frequent post-earthquake floods described later in this report, may have similarly deposited sediments in the shorefront areas. In addition to ejecta, other indications of liquefaction included building settlement, lateral spreading, wharf and seawall collapse, and other ground disturbances (e.g., rolled curbs, deformed sidewalks).

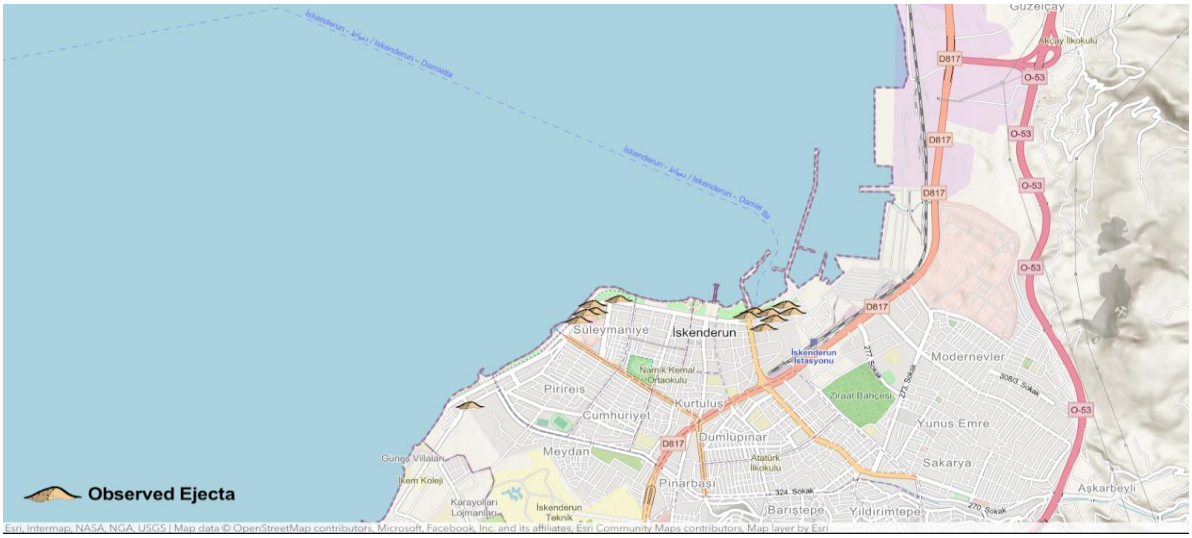

Figure 2.1. Areas visited between February 26 and March 5 (Phase 2) where liquefaction-induced hazards were observed (from GEER / EERI LFE 2023).

The areas of liquefaction in İskenderun appear to be associated with reclaimed land and land near the pre-development shoreline. As a port city, İskenderun was largely developed in the 19th and 20th centuries. Historic documents (i.e., maps from 1851, 1872 and 1896, which were obtained from the General Directorate of State Archive of Prime Ministry and compiled in Nalça 2018) describe the area as marshy, with streams flowing from the mountains in the east into İskenderun. Development efforts included building drainage canals, filling in the low-lying marsh areas, and reclaiming land along the shoreline.

The approximate İskenderun shorelines in 1916 and 1928, based on historic maps compiled by Nalça (2018), are shown in Figure 2.2. Figure 2.2 also shows the two historic maps of İskenderun (historically called Alexandretta) from 1916 and 1928 that were used to approximate the historic shorelines. The İskenderun shoreline was built out during the city's development. Present-day Atatürk Boulevard has a similar alignment to the shoreline from the 1916 map, representing the approximate border between reclaimed and naturally-formed land. Documents of the development of the İskenderun shoreline, compiled in Nalça (2018), provide a basis to delineate potential subsurface constraints on the extent of liquefaction and lateral spreading failure. Several past post-earthquake case studies have similarly shown a correlation between the spatial extents of liquefaction and areas of anthropogenic fills, including the San Francisco shoreline in the 1989 Loma Prieta earthquake (Pease & O'Rourke 1997), port and harbor facilities in the 1995 Kobe earthquake (Ishihara et al. 1996), and the Tone river in the 2011 Tohoku earthquake (Pradel et al. 2014).

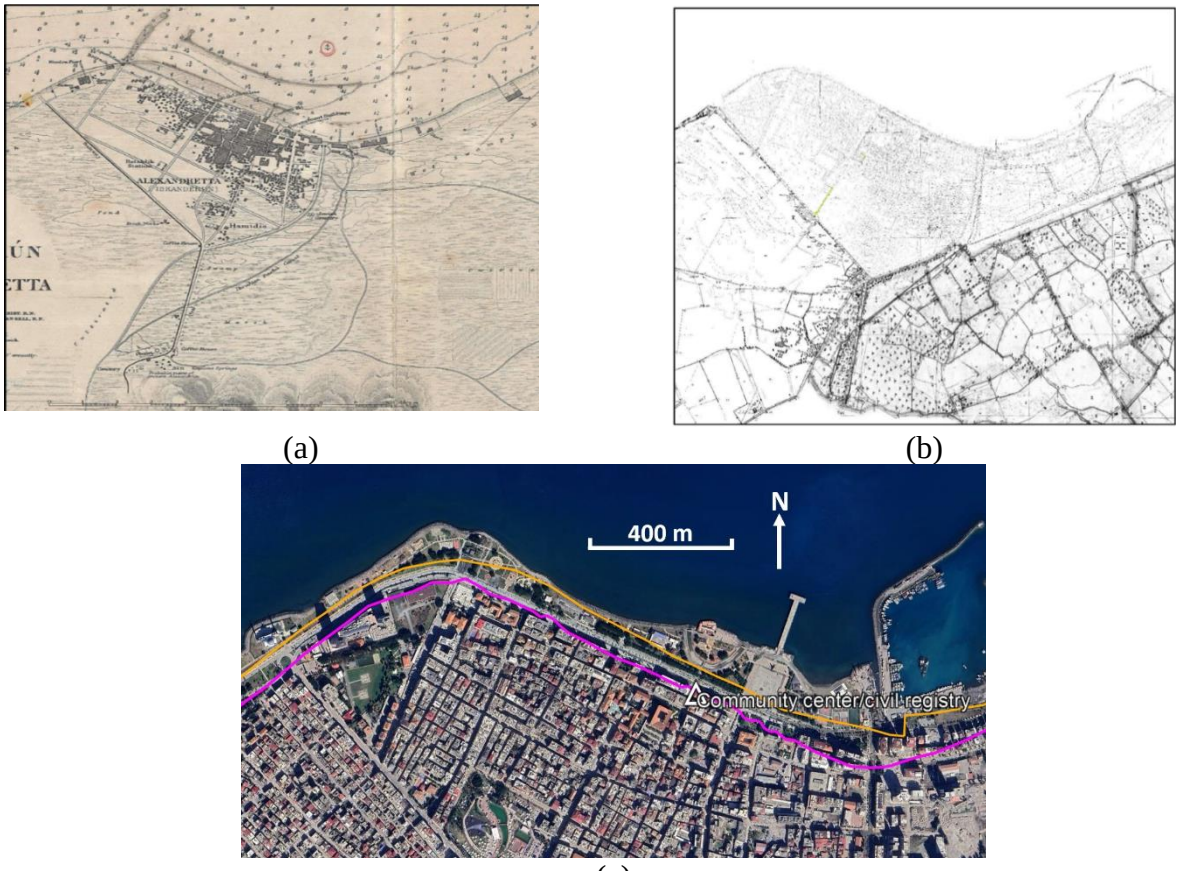

Figure 2.2. Shoreline history in İskenderun: (a) historic map from 1916 (source Hrt 1994 D 859, National Library of Türkiye, obtained from Nalça (2018)), (b) compiled historic map from 1928 from Nalça (2018), and (c) current day İskenderun with the approximate historic shorelines from 1916 (pink line) and 1928 (orange line); the location of the community center / civil registry in Figure 2.3 is indicated for comparison. Base image obtained from Google Earth© (dated 16-February-2023).

An example of this shoreline development is shown in Figure 2.3. The two photos show the same building, a former community center and current civil registry (36.5916N, 36.1702E; all GPS coordinates are given in decimal degrees). The historic photo in Figure 2.3a, which pre-dates 1916 (although the year it was taken is unknown), shows the community center along the former shoreline of İskenderun. The modern image of the same building in Figure 2.3b shows the development of reclaimed land that has pushed the shoreline out.

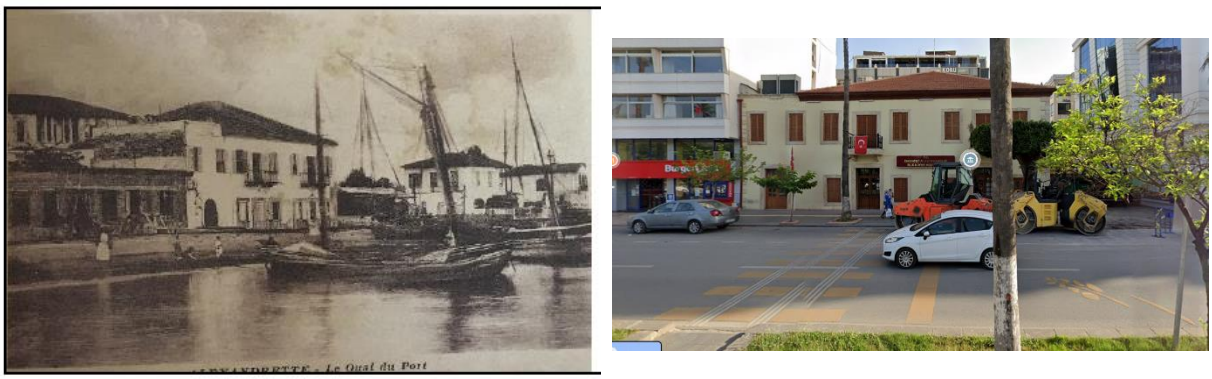

(a) (b)

Figure 2.3. İskenderun shoreline: (a) historic photo of the former community center and current civil registry located at 36.5916N, 36.1702E [the photo pre-dates 1916, is credited to Köker, Musa Dağı Emenileri, 69, and was obtained from Nalça (2018)]; (b) modern image of the civil registry building obtained from Google Street View© (image capture May 2020).

Residents of İskenderun reported regular flooding in the waterfront areas, including the Çay district, following the February 6 earthquakes. These reports from residents were consistent with observations by the GEER Phase 3 team of several owners pumping water from their basements in the Çay district. The owner of No. 28 Bahçeli Sahil Evler Street, Ahmet Palalıoğlu, explained that he was sealing off the basement windows to his apartment building due to the regular flooding. Additionally, standing water was seen along the edges of buildings along Atatürk Boulevard between 41. Sk. and Ziya Gokalp Street (approximately 36.5916N, 36.1706E) on March 28.

The GEER Phase 3 team observed notable flooding that took place on March 29, 2023 (Figure 2.4). On this day there was heavy rainfall and strong onshore winds in the İskenderun area. The flooding was observed from the Çay district and southeast along Atatürk Boulevard and the shoreline to past Mithatpaşa Street. The photos show that flooding advanced at least two roads in from the shoreline, including past Mareşal Fevzi Çakmak Street (Figure 2.4a), and past Bahçeli Sahil Evler Street (Figure 2.4b) in the Çay district. The team returned to İskenderun and Çay on April 1, 2023 when flooding had largely subsided, however, significant standing water remained. Drone footage taken on April 1 with observations of standing water in the Çay district is shown in Figure 2.5.

(a) (b) (c)

Figure 2.4. Flooding in İskenderun, Hatay: (a) (36.5912N, 36.1698E; 29MAR2023) flooding in a commercial district (b) (36.59102N, 36.1792E; 29MAR2023) flooding in the Çay district, (c) (36.5922N, 36.1687E; 29MAR2023) flooding of Atatürk Boulevard, near a commercial district.

(a) (b)

Figure 2.5. Remnant flooding in İskenderun, Hatay captured from drone footage on April 1, 2023. Red-roofed building marked with a red "X" for reference. (a) (approx. 36.5900N, 36.1773E) (b) (36.5901N, 36.1783E).

Damage to the shoreline and water distribution infrastructure, as well as liquefaction-induced ground settlement and lateral spreading over a large area of the waterfront of İskenderun, are all postulated as potential contributing factors to the more frequent flooding since the 2023 earthquakes. The GEER Phase 1 team collected reports there was a broken water main in İskenderun. The GEER Phase 3 team noted potential settlement of a rubble mound sea wall. Change detections of Synthetic Aperture Radar (SAR) images suggests that İskenderun has been continually subsiding over the four years prior to the earthquake at rate of over 40 mm/year (Papageorgiou et al. 2023). Additional investigations are anticipated to investigate further the cause of flooding following the earthquakes.

2.1.2 Gölbaşı, Adıyaman

Gölbaşı is located along the Lake Gölbaşı (Gölbaşı Gölü) in the province of Adıyaman. Evidence of liquefaction was observed throughout the town by the GEER Phase 1, Phase 2, and Phase 3 teams. Evidence of liquefaction included ejecta, building settlement, and lateral spreading. Lateral spreading around the lake and its impacts on infrastructure was surveyed by the GEER Phase 2 team. The METU team, led by Prof. K. Onder Cetin, is continuing to perform surveys of liquefaction-induced building settlement and liquefaction occurrence in Gölbaşı. Examples of the building damage and ground deformations observed in Gölbaşı are shown in Figure 2.6.

Eight samples of liquefaction ejecta were collected by the GEER Phase 3 team on March 30, 2023. The sample locations and sample numbers are indicated in Figure 2.7. The ejecta samples were characterized in the ZETAŞ geotechnical laboratory. The measured Atterberg Limits, fines content (percentage of sample by mass < 0.075 mm), proportion of sand (≥ 0.075 mm, and < 4.75 mm), and gravel content (≥ 4.75 mm) are summarized in Table 2.1. The measured plasticity index (PI) is between 9 and 14, with fines content between 18% and 52%. The METU team also collected samples of liquefaction ejecta in Gölbaşı during March 30, 2023 at similar locations. Their testing indicated PI values varying the range of 16 to 23, as shown in the parentheses in Table 2.1. Additional testing of ejecta samples will be performed to investigate the discrepancies in index values further. Moreover, as part of the follow up studies, intact samples are to be retrieved which will help more accurately identify the critical layers and sources of ejecta.

(a)

(b)

(c)

Figure 2.6. Reconnaissance photos in Gölbaşı, Adıyaman (a) (37.7874N, 37.6430E; 30MAR2023) building tilting and settlement, and road cracking, (b) ground and sidewalk disturbance (37.7979N, 37.6430E; 30MAR2023), and (c) ejecta (37.7877N, 37.6430E; 30MAR2023).

Table 2.1. Summary of test results on ejecta collected from Gölbaşı, Adıyaman.

Sample name	Northing	Easting	Liquid Limit	Plastic Limit	Plasticity Index	Fines Content (%)	Sand Content (%)	Gravel Content (%)
WP-38	37.787687	37.643042	29[a] (35)[b]	18 (15)	11 (20)	35 (33)	64 (64)	1 (0)
WP-41	37.788049	37.642052	32 (32)	19 (16)	13 (16)	52 (33)	48 (67)	0 (0)
WP-45	37.788386	37.641917	31	17	14	42	57	1
WP-47	37.788685	37.641998	28 (32)	19 (15)	9 (17)	18 (22)	77 (68)	5 (0)
WP-49	37.788774	37.640507	29 (35)	19 (16)	10 (19)	23 (35)	77 (64)	0 (1)
WP-50	37.788476	37.640745	28	18	10	35	65	0
WP-51	37.789188	37.642871	30 (35)	19 (16)	11 (19)	44 (46)	56 (52)	0 (2)
WP-52	37.789799	37.644325	32 (42)	19 (19)	13 (23)	40 (58)	59 (40)	1 (2)

[a] Values outside of parentheses indicate those obtained from testing in the ZETAŞ soil laboratory.

[b] Values in parentheses indicate those obtained from testing in the METU soil laboratory.

Figure 2.7. Locations and sample numbers of ejecta sampled in Golbaşi on 30MAR2023. Base image from Google Earth©dated 6MAR2023. Approximate center of the image is (37.7884N, 37.6428E).

2.1.3 Antakya, Hatay

Antakya, Hatay is located near the ancient city of Antioch built around 300 BC along the Orontes River. Antioch has been damaged by several large earthquakes throughout its long history. Figure 2.8 shows one of several depictions of the historic city, including a former path of the

Orontes River (Uggeri 1998). Although subject to interpretation, this map suggests a different river path than the river that currently runs through the modern day city.

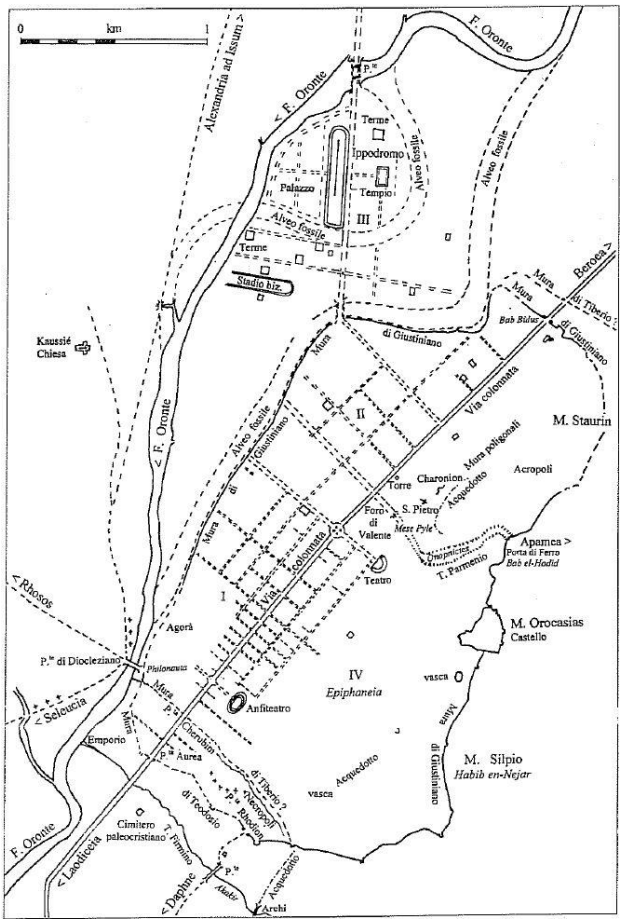

Figure 2.8. Interpreted map of the ancient city of Antioch, near modern-day Antakya (Uggeri 1998).

Antakya was visited on March 31, 2023. Satellite images of the Orontes River north of Antakya showed evidence of liquefaction and lateral spreading from the February earthquakes (e.g., Taftsoglou et al. 2023). Furthermore, liquefaction was observed by the GEER Phase 1 team at Hatay Airport. Despite this evidence of liquefaction around Antakya, the GEER Phase 3 team did not observe clear evidence of liquefaction in the areas visited in and around Antakya, besides riverbank slope failures that may or may not have been liquefaction induced. The route and locations visited are shown in Figure 2.9. There was widespread and devastating structural damage in Antakya. Structural and geotechnical damage at and near selected bridges was documented by the GEER Phase 3 team in Antakya and is described in Section 4.

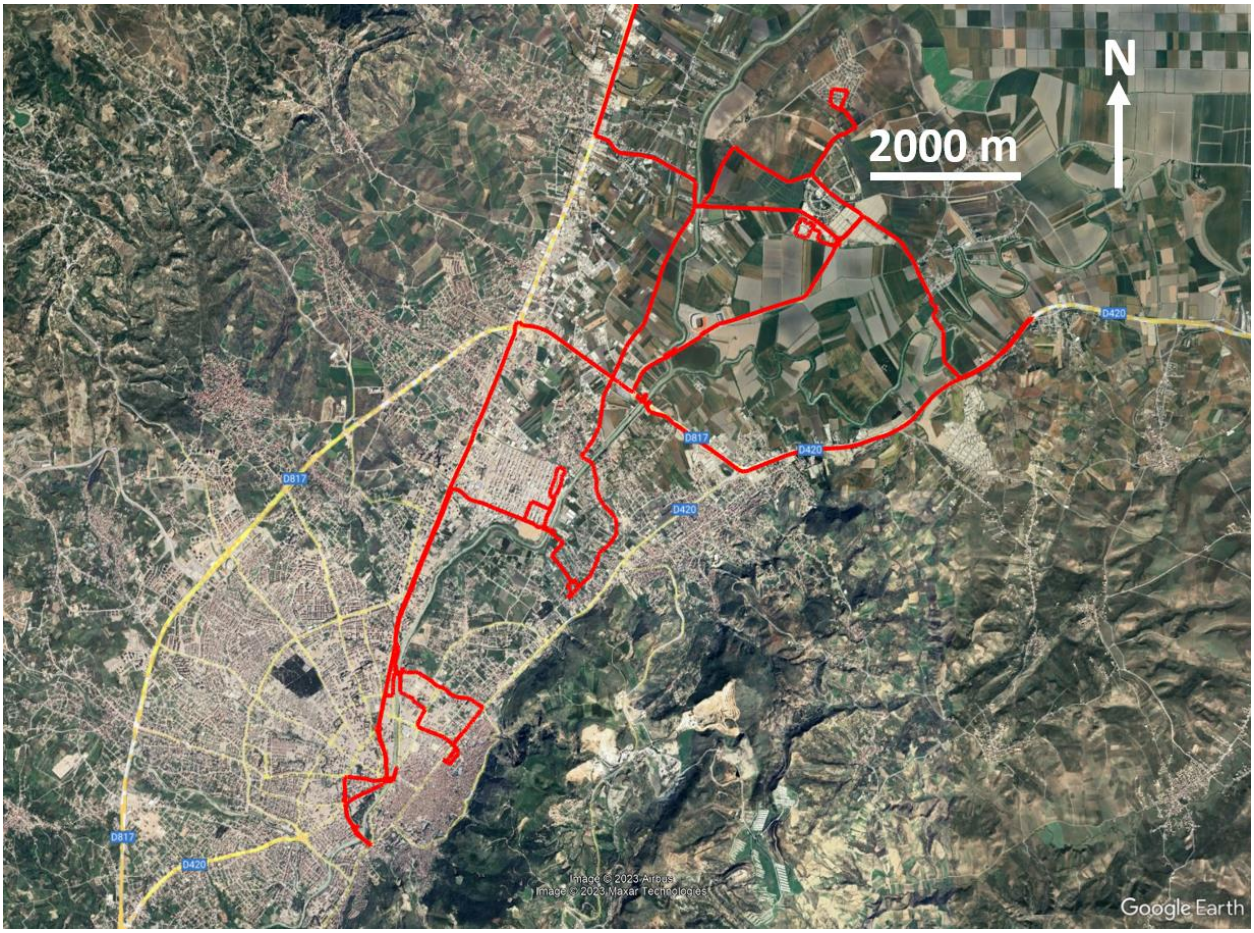

Figure 2.9. GPS track of the areas visited by the GEER Phase 3 team in and around Antakya, Hatay. No clear evidence of liquefaction was observed at these locations. (Google Earth© image dated May 8, 2023, centered near 36.2385N, 36.2385E).

2.2 Lateral Spreading

2.2.1 İskenderun, Hatay - General Spreading

The GEER Phase 3 team obtained detailed measurements of lateral ground displacements at lateral spread sites along seven transects perpendicular to the İskenderun shoreline. Four of the transects labeled as LS-1 to LS-4 were taken directly from the waterfront and are documented herein. A map depicting the transect locations of LS-1 to LS-4 is presented in Figure 2.10 below. Three other transects labeled as LS-5 to LS-7 were taken in the Çay District near buildings with noticeable settlement and are presented in Section 2.2.2 of this report.

Figure 2.10. Map of measured lateral spread locations (LS-1 to -4) extending from the seawall in İskenderun, Hatay Province, Türkiye (Google Earth© image dated February 16, 2023, centered near 36.5928N, 36.1632E).

The lateral spreading transects were measured by taking the distance from a set datum (e.g., inside of waterfront seawall) to all observed cracks along that line. The widths of all crack openings were measured and accumulated along each transect, in a manner similar to the methodology of Robinson et al. (2010) used in the 2010 Darfield earthquake in Christchurch, New Zealand. The transect locations were chosen to coincide typically with long stretches of concrete blocks and pavement, where crack openings were easier to identify (i.e., not obscured by vegetation) and relatively unaffected by water action from the floods that occurred since the earthquake events.

The measurements were taken on March 28 and April 1 of 2023. A rainstorm occurred on March 29 that caused extensive flooding, inundating several city streets over 200 m from the waterfront. Possible differences along the shoreline, before and after this flooding event, are presented herein.

Figures 2.11 to 2.14 depict photos of each lateral spreading transect. LS-1 (start point: 36.59360N, 36.15846E) was taken about 100 m to the east of the Nihal Atakaş Camii mosque as depicted in Figures 2.11a-d. As observed from a series of past Google earth satellite images, the mosque appears to be built over recently infilled land, and construction was likely completed in 2018. However, the transect extends through previously existing ground along the shoreline. The transect starting point was taken at a rubble mound seawall that was observed to have a reduced height of 0.5 to 0.8 m relative to the seawall directly in front of the mosque (Figure 2.11a). The transect extended to the south end of Atatürk Blvd. Significant extensional cracks along the shoreside pedestrian path, grass field, and Atatürk Blvd were documented (Figure 2.11b-c), suggesting a total horizontal ground movement of about 54 cm. The overall extent of this spread to the south may have been constrained by the İskenderun Park Forbes AVM shopping mall.

(a)

(b)

(c)

(d)

Figure 2.11. Photos of lateral spread LS-1: (a) observed 0.5 to 0.8 m reduction in height of rubble mound seawall at start of LS-1 relative to infilled area of Nihal Atakaş Camii mosque (36.5936N, 36.1583E; 28MAR2023), (b) pavement tile separation near shorefront (36.5933N 36.1581E; 28MAR2023), (c) pavement crack extending along southwest bound portion of Atatürk Blvd (36.5930N, 36.1588E; 28MAR2023), and (d) separation between curb and bike lane (36.5934N, 36.1587E; 28MAR2023).

LS-2 (start point: 36.59358N, 36.16731E) was taken along the east side of the Doĝan restaurant 1-story patio building as depicted in Figures 2.12a-d. The patio building was not being used, likely due to severe ground cracking within the building and around its exterior. The transect was taken from just inside the seawall behind the building to just south of the main 2-story restaurant building, which appeared structurally sound, but was also not in service. The measured cracks were taken along the concrete pathway adjacent to the restaurant buildings, accumulating to about 76 cm of total lateral movement. Cracking along the base of the patio building wall and extending

guardrail wall approximately matched the adjacent ground cracking at LS-2, with a 30 cm lateral extension over a distance of 19 m along the walls (i.e., extensional strains of over 1.5%).

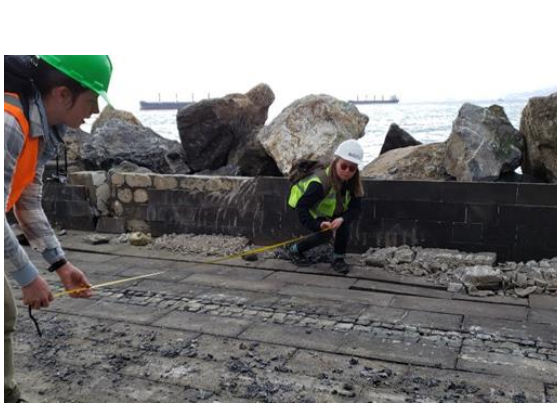

(a)

(b)

(c)

(d)

Figure 2.12. Photos of lateral spread LS-2: (a) seawall at start of LS-2 (36.5937N, 36.1672E; 01APR2023), (b) sunken park bench and spreading along eastern wall of Dogun restaurant patio (36.5937N, E36.1672E; 01APR2023), (c) cracks near column at southeast corner of patio (36.5934N, 36.1672E; 01APR2023), and (d) cracking along back of patio (36.5935N, 36.1671E; 01APR2023).

LS-3 (start point: 36.59355N, 36.16742E) was taken about 10 m to the east of LS-2, over a similar north to south extent, as depicted in Figures 2.13a-b. The purpose of this transect was to understand whether LS-2 was influenced by the structural performance of the patio foundation. The accumulated lateral spreading measured over LS-3 was about 72 cm and followed a consistent spreading trend with distance from the seawall as LS-2.

(a)

(b)

Figure 2.13. Photos of lateral spread LS-3 (10 m east of LS-2): (a) seawall at start of LS-3 (36.5934N, 36.1668E; 01APR2023), and (b) walkway at end of LS-3 (36.5931N, 36.1673E; 01APR2023).

LS-4 (start point: 36.59326N, 36.16883E) was measured initially on March 28 and then again on April 1, 2023. It is depicted in Figures 2.14a-b. The transect extended from inside the seawall to a pedestrian pathway just north of and parallel to Atatürk Blvd. The transect was measured along a tiled concrete walkway perpendicular to the shoreline. The accumulated lateral spreading measured over LS-4 during our visit on March 28 was about 140 cm. During our visit on April 1 (three days after the March 29 storm event), it was observed that the seawall rubble was about 1 m higher and the reinforced concrete parapet wall behind the rubble was much more heavily damaged. Construction equipment wheel tracks were also observed along the waterfront in this area. It is believed that additional rubble was placed for temporary flood mitigation and protection

against future storms. Our measurements indicate that lateral displacements increased by about 7 cm over the intervening period. Despite potential uncertainties in our measurements, this may have been caused by movement or vibrations from heavy machinery used to place the rubble, scour and movement of surficial features (e.g., concrete pavement blocks) during the March 29 storm, or additional ground movements occurring since the previous measurements.

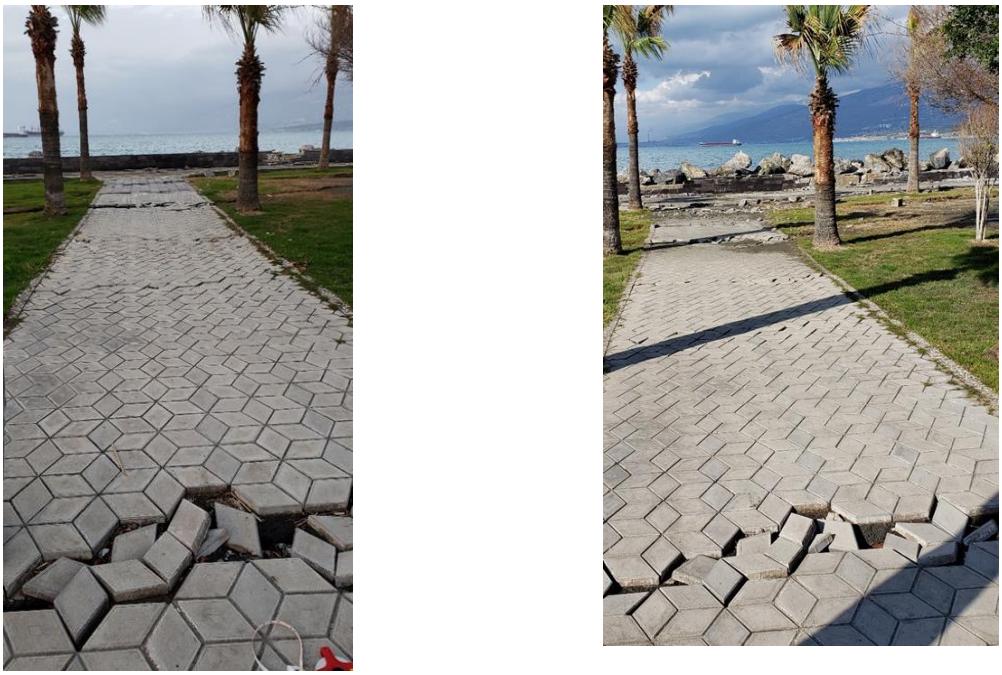

(a) (b)

Figure 2.14. Photos of lateral spread LS-4 along tiled concrete walkway: (a) before the March 29, 2023 storm event (36.5930N, 36.1687E; 28MAR2023), and (b) three days after the March 29, 2023 storm event (36.5930N, 36.1687E; 01APR2023). Notice damage to seawall and higher rubble mound in more recent photo, presumably caused by additional rubble placement in the intervening time between photos.

Figure 2.15 depicts the accumulated measured lateral displacement along each transect from the shoreline. The maximum lateral ground movements at the shoreline for these four transects varied from 50 to 150 cm. Lateral ground displacements could be observed up to distances of 40 to 65 m from the shoreline. It is of interest to note that the distribution of lateral ground movement with distance from the shoreline is generally constant over the length of each measured transect (i.e., the change in the accumulated lateral displacement over equal increments of distance from the seawall is relatively constant). However, the rate of change of the accumulated lateral displacement over equal increments of distance from the seawall of each of the transects varies.

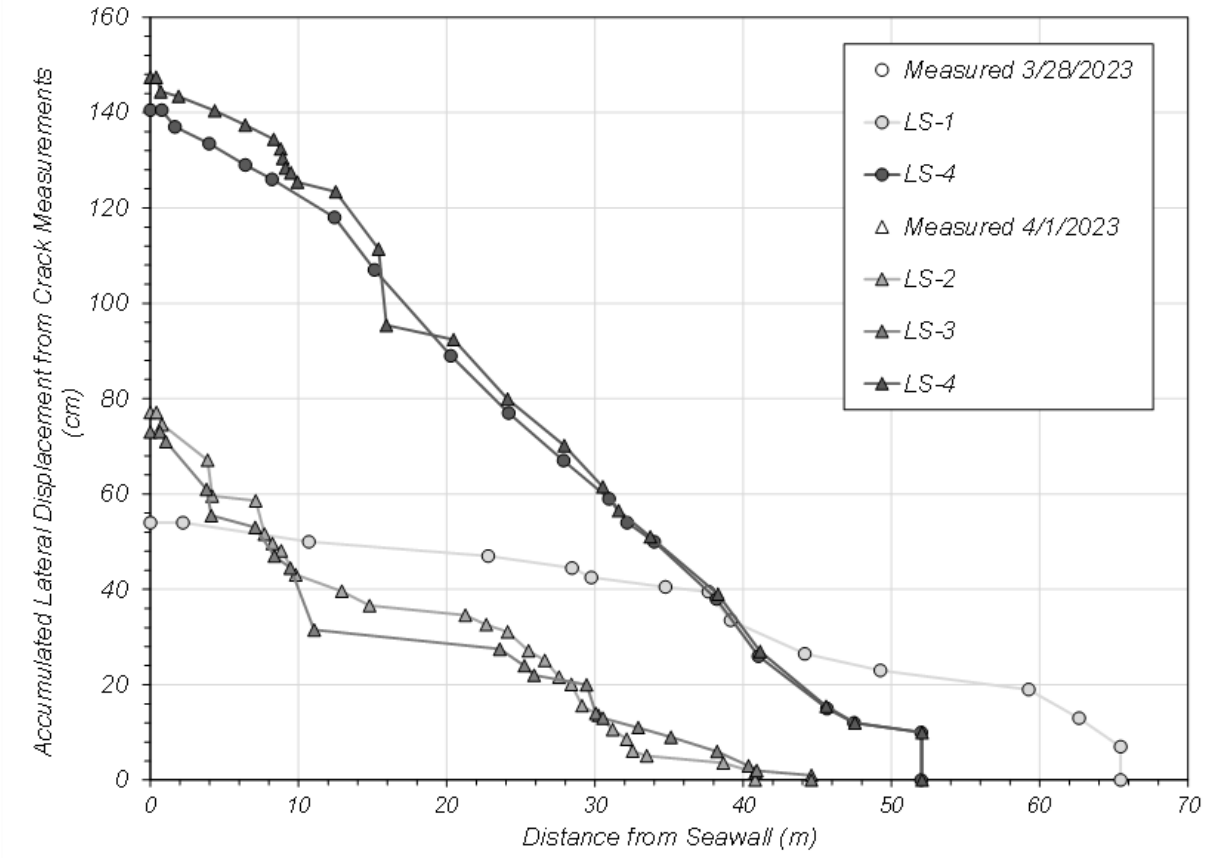

Figure 2.15. Accumulated lateral displacements as measured from crack opening widths along LS-1 to LS-4 relative to distance from the seawall in İskenderun.

2.2.2 İskenderun, Hatay - Near Çay District Buildings

Lateral spreading was measured by the GEER Phase 3 team along three transects near Çay district buildings in İskenderun from March 28 to April 1, 2023. The purpose of these measurements was to check the total local displacement relative to adjacent buildings that were also observed to settle (i.e., the buildings described in Section 3.1.1). These measurements can help indicate whether the cracks observed adjacent to the buildings primarily occurred due to vertical building movements (i.e., settlement-induced ground extension) or global lateral movements (i.e., lateral spreading as observed along the İskenderun shoreline and described in Section 2.2.1 of this report). The transects, labeled as LS-5 to LS-7, are shown in Figure 2.16. Measurements were taken using the same procedure described in Section 2.2.1.

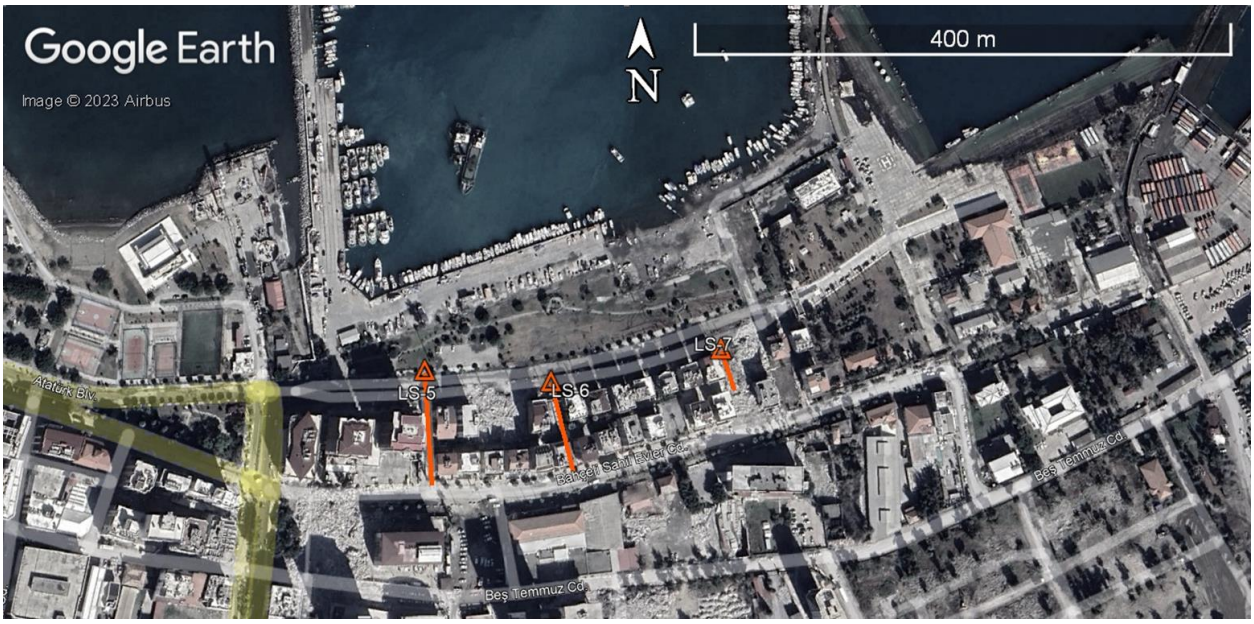

Figure 2.16. Map of measured lateral spread locations (LS-5 to LS-7) extending from Atatürk Boulevard in the Çay district of İskenderun, Hatay Province, Türkiye (Google Earth© image dated February 16, 2023, centered near 36.5906N, 36.1784E).

As depicted in Figure 2.16, transects LS-5 to LS-7 did not extend to the shoreline. This was due to the GEER team's inability to access the boat dock, and the difficulty of detecting cracks within the adjacent grassy park that may have been obscured following recent floods. However, significant spreading likely occurred shoreward of the measured transects, as evidenced by ground cracks and preserved sand boils observed in the grassy park and extensional cracking observed along the perimeter of the boat dock as shown in Figure 2.17. The documented cracks were visible along the paved ground in the vicinity of the buildings of interest.

Figure 2.17. Sand boils and lateral spreading near boat dock in Çay district of İskenderun, Hatay Province, Türkiye (36.5915N, 36.1789E; 01APR2023).

Figures 2.18 to 2.20 depict photos along each lateral spreading transect. LS-5 (start point: 36.59081N, 36.17679E) extended from the north side of Atatürk Blvd to Bahçeli Sahil Evler Street just south of the inspected block of 5-story buildings. Ground cracks observed along Atatürk Blvd were primarily oriented parallel to the shoreline, however, transverse cracking and the formation of separated blocks were also observed across the roadway (e.g., Figure 2.18a). South of Atatürk Boulevard, transect LS-5 extended along a paved path between a relatively stable 7-story building to the west, and the 5-story block of buildings that settled to the east. LS-6 (start point: 36.59073N, 36.17781E) extended from the south side of Atatürk Blvd to Bahçeli Sahil Evler Street. A majority of the transect was taken within the alley between the Pallet Hookah building and three 5-story buildings that had settled (Section 3.3.1f). LS-7 (start point: 36.59093N, 36.17918E) extended from the south side of Atatürk Blvd to the north edge of building No. 14 Bahçeli Sahil Evler Street and runs along the east side of the group of four buildings (Section 3.1.1g).

(a)

(b)

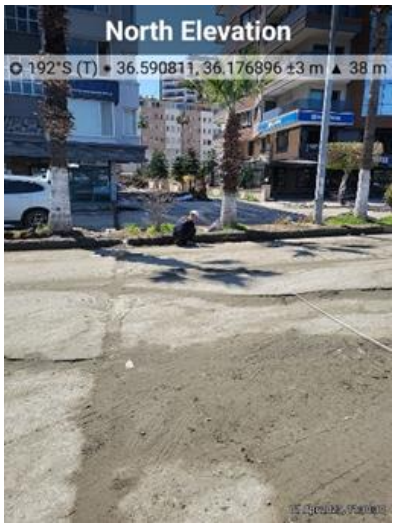

(c)

(d)

(e)

Figure 2.18. Photos of lateral spread LS-5 taken April 1, 2023: (a) start of LS-5 at north sidewalk curb along Atatürk Blvd (36.5908N, 36.1769E; 01APR2023), (b) separated pavement block with 3 to 6 cm of vertical displacement bounded by horizontal cracks of 10 to 20 cm along Atatürk Blvd (36.5908N, 36.1767E; 01APR2023), (c) cracks along Atatürk Blvd (36.5908N, 36.1769E; 01APR2023), (d) 5 cm crack aligned with front edge of building foundations along Atatürk Blvd (36.5906N, 36.1768E; 01APR2023), and (e) minor cracking along end of LS-5 (36.5903N, 36.1767E; 01APR2023).

(a)

(b)

(c)

(d)

Figure 2.19. Photos of lateral spread LS-6: (a) start of LS-6 at south sidewalk along Atatürk Blvd in front of building Belli Apartment #18 (36.5907N, E36.1778E; 29MAR2023), (b) cracking along wall behind buildings (36.5904N, 36.1778E; 29MAR2023), (c) cracking along wall behind buildings (36.5905N, 36.1779E; 28MAR2023), and (d) end of LS-6 along the side of building Kaan Ela #24 (36.5905N, 36.1779E; 29MAR2023).

(a) (b)

Figure 2.20. Photos of lateral spread LS-7 (a) minor cracking along east side of settled building (36.5907N, 36.1791E; 01APR2023), and (b) cracking along courtyard behind buildings (36.5911N, 36.1789E; 01APR2023).

Figure 2.21 depicts the accumulated measured lateral displacement along each transect (i.e., y-axis) relative to their distance from the shorefront (i.e., x-axis). While the full extent of spreading between the shoreline and the buildings (i.e., between about x = 0 and 100 m) could not be measured, it is believed to have been greater than 50 cm at all transects. Ground cracks were highly concentrated within the alley behind the two rows of 5-story buildings (i.e., between about x = 120 and 140 m), suggesting over 20 cm of lateral extension in this area for LS-6 and LS-7. LS-5 depicted more gradual cracking along the building alley, which could potentially be attributed to the stable 7-story building redistributing the crack patterns in this area. With the current information, it remains difficult to speculate whether the cracks between buildings resulted from building settlement, overall seaward lateral spreading, or a combination of both mechanisms. Additional insights from remote sensing change detections, subsurface data, computational analyses, and other evaluations may help clarify the global picture of damage in this area.

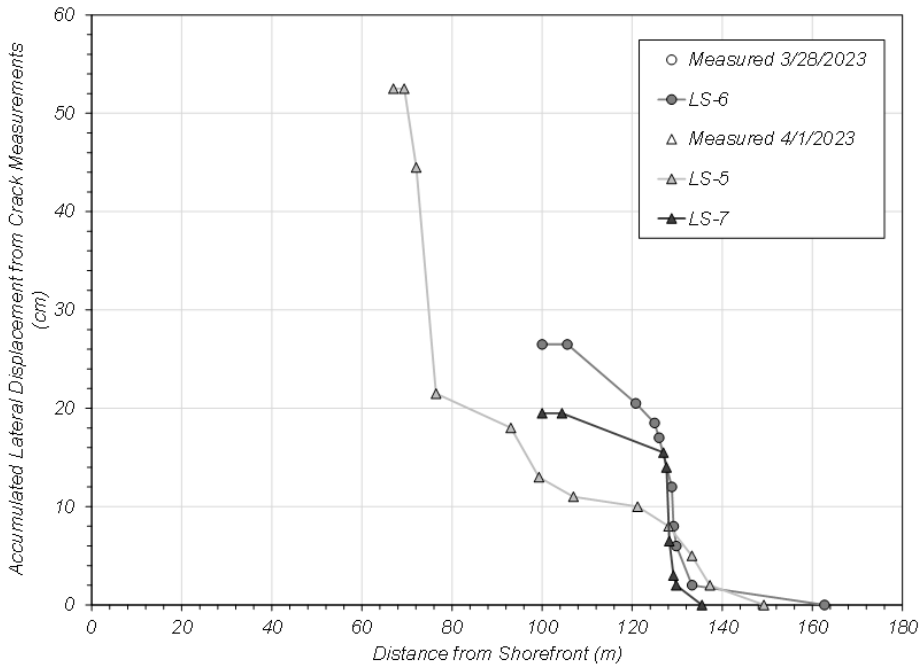

Figure 2.21. Accumulated lateral displacements as measured from crack widths along LS-5 to LS-7 relative to distance from the approximate shorefront of the Çay district in İskenderun.

2.3 Fill Settlement

2.3.1 Hospital, Antakya, Hatay

The GEER Phase 3 team visited the Hatay Egitim ve Arastirma Hastanesi (hospital) in the Antakya, Hatay Province region to observe the geotechnical engineering aspects of its seismic performance. The hospital was closed due to structural damage and the parking lot was being used as a temporary field hospital for earthquake survivors at the time of the GEER visit on March 31, 2023.

The hospital appears to be composed of several structures connected by walkways. Google earth images indicate that hospital construction started between 2013 and 2014. Reconnaissance included walking the perimeters of the hospital buildings and taking measurements and pictures to document fill settlement and other damage. The team did not enter the buildings. An aerial image of the hospital area is shown in Figure 2.22 with “A”, “B”, “C”, and “D” put on the photo to indicate areas being referenced in the reconnaissance description. The compacted earth fill settled relative to the hospital building throughout its perimeter, exceeding 48 cm in some areas. Some of the pipelines and utilities connected to the building were damaged due to this difference in settlement. Several of the entrances into the hospital structures were damaged due to the ground settlement, which limited access to and from the hospital. The hospital and surrounding parking lot and facilities appear to be built over compacted earth fill, due to their higher elevation than the

surrounding valley. It is believed that the hospital's foundation system extended to stronger material beneath the surrounding earth fill that settled, presumably due to earthquake shaking.

Area "A" is the north side of the north building and appeared to be the main hospital entrance. An overview of this area is shown in Figure 2.23a, including some pavement damage. Closer inspection of the ground close to the structure resulted in measurements of fill settlement from 0 cm to 48 cm. Figure 2.23b pictures an entrance ramp where 48 cm of fill settlement was measured between the entrance and the top of the ramp. Figure 2.23c pictures the ground near the base of the ramp where 0 cm to 18 cm of fill settlement was measured. Figure 2.23d shows another entrance where there was damage to the pavement and stairs.

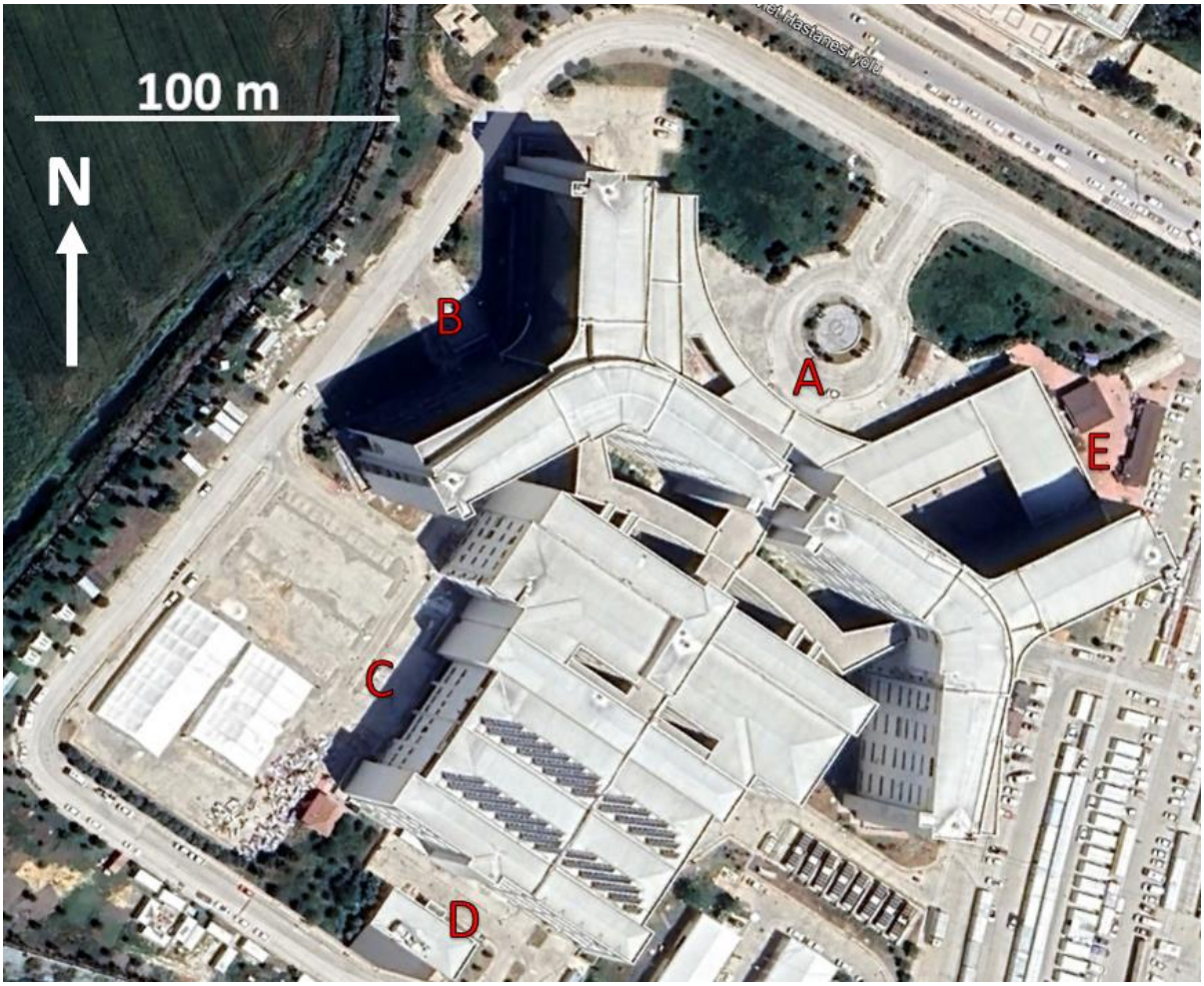

Figure 2.22. Aerial photo of the hospital perimeter surveyed for geotechnical damage. The approximate center of the image is (36.2700N, 36.2240E). Image dated 8MAY2023 and obtained from Google Earth©.

(a) (b)

(c) (d)

Figure 2.23. Fill settlement on the north side of the main hospital building (area "A" in Figure 2.22): (a) overview of north-facing front of hospital showing some pavement damage (36.2709N, 36.2241E; 31MAR2023), (b) settlement of an entrance ramp about 48 cm relative to the structure and entrance (36.2705N, 36.2244E 31MAR2023), (c) 0 cm to 18 cm of fill settlement relative to the structure (36.2704N, 36.2245E, 31MAR2023), and (d) damage to pavement and stairs at an entrance (36.2709N, 36.2239E, 31MAR2023).

Area "B" is the west side of the north hospital building. Damage to utility connections, likely due to differential fill settlement, was also documented in this area. Figure 2.24a shows an overview of this area including an entrance and a landscaped area. Notable settlements and damage to stairs at the entrance was documented by the picture in Figure 2.24b. There were notable differences in settlement measured between the concrete and grass areas. These deformations also opened up a

gap between the concrete and grass areas, and exposed damaged utility connections (Figures 2.24c,d). The differences in settlement were measured to be 30 to 40 cm, and the opening between the concrete and grass was measured to be up to about 10 cm.

(a)

(b)

(c)

(d)

Figure 2.24. Fill settlement on the east side of the main hospital building (area "B" in Figure 2.22): (a) view of the east side (36.2711N, 36.2234E, 31MAR2023), (b) damage to entrance stairs (36.2707N, 36.2233E; 31MAR2023), (c) different settlements between the concrete and grass area exposing damaged utility connections (36.2704N, 36.2230E, 31MAR2023), and (d) different settlements between the concrete and grass area exposing utility connections (36.2704N, 36.2231E, 31MAR2023).

Area “C” includes the south structures of the hospital. Damaged structures in Area C are shown in Figure 2.25a with some evidence of fill settlement. Notable fill settlement was observed near the structure shown in Figure 2.25b. This settlement appears to be focused in an area of utility connections. Although utility lines are exposed in this area, it is not known if they were exposed due to damage or to support the field hospital operations set up in the main parking lot.

(a) (b)

Figure 2.25. Fill settlement and damage on the east side of the southside hospital structures (area “C” in Figure 2.22): (a) view of damaged buildings (36.2703N, 36.2229E, 31MAR2023), and (b) fill settlement and exposed utility lines (36.2698N, 36.2228E, 31MAR2023).

Area “D”, which is the south side of the hospital structures, appeared to be the emergency services entrance. The emergency services entrance is shown in Figure 2.26. The settlement in this area was measured as up to 40 cm.

(a) (b)

Figure 2.26. South side of the hospital (area “D” in Figure 2.22): (a) overview of the south side (36.2691N, 36.2234E, 31MAR2023), and (b) ambulance entrance where up to 40 cm of fill settlement was measured (36.2691N, 36.2234E, 31MAR2023).

Area “E” is the west side of the northside hospital structures. The ground in this area is finished with paver tiles. Ground openings were measured in this area, with the opening at one point measured to be 32 cm wide, 47 cm deep and having 8 cm of settlement.

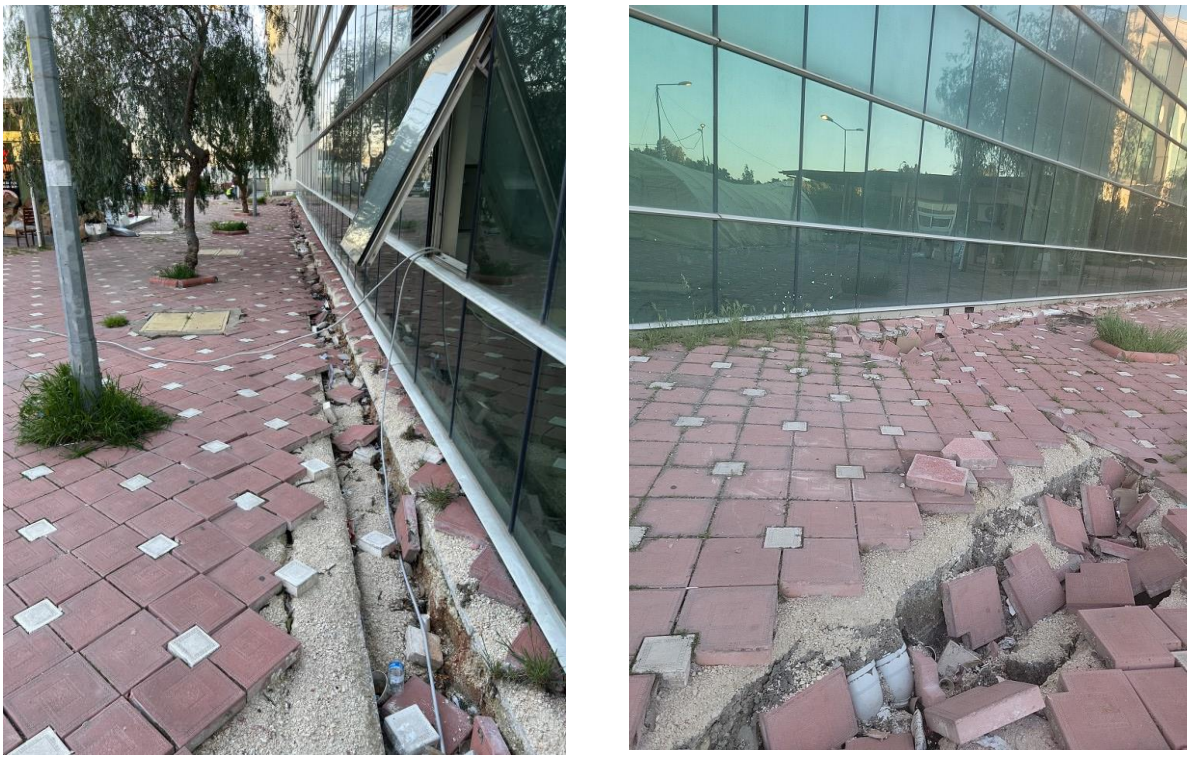

(a) (b)

Figure 2.27. West side of the northside hospital structure (area “E” in Figure 2.22): (a) fill settlement along the structure (36.2706N, 36.2250E, 31MAR2023), (b) fill settlement and ground opening (36.2703N, 36.2252E, 31MAR2023).

3. BUILDING SETTLEMENT, TILTING, AND INTERACTIONS

3.1 İskenderun, Hatay

The GEER Phase 3 team documented building settlements in İskenderun on March 27, 28, 29 and April 1, 2023. The GEER Phase 3 team survey included a range of building settlements from negligible settlement to greater than 70 cm of settlement. Interactions of building settlements and ground deformations at groups of buildings were also observed. Data was collected through hand-survey measurements, terrestrial lidar scans (FARO Focus3D X 330 2014), and photographs. The GEER Phase 3 team documented the seismic performance of 22 buildings in İskenderun, of which there were three clustered building groups where interactions between buildings were observed and documented.

3.1.1 Çay District

The buildings surveyed in the Çay district are shown in Figure 3.1. The numbers on the buildings in the figure represent the street address number. Lidar scans were performed at some of the surveyed buildings. The approximate location of the lidar scans are shown in the figure with the scan number for reference. This report details the measured building settlements and a preliminary analysis of the lidar data.

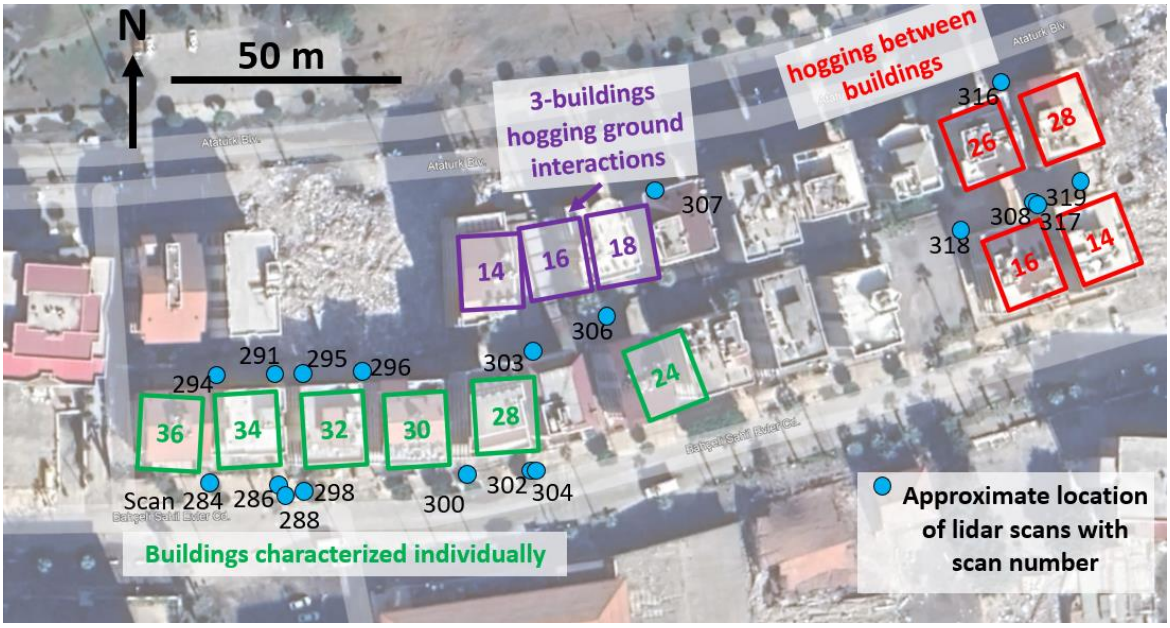

Figure 3.1. Location of the surveyed buildings by the GEER Phase 3 team in the Çay district of İskenderun with approximate locations of lidar scans. Approximate location of the middle of the figure is 36.5906N, 36.1780E; base image from Google Earth© dated February 16, 2023. The numbers within the building footprints are building address numbers.

(a. Çay) No. 34 Ersoz, Bahçeli Sahil Evler Street

The residential apartment building No. 34 Ersoz located on Bahçeli Sahil Evler Street (36.5902N, 36.1772E) was surveyed on March 27, 2023. This building and the nearby Building No. 36 were surveyed previously by the GEER Phase 2 team. The street-view of Building No. 34 is shown in Figure 3.2a; a view of the rear of the building is shown in Figure 3.2b. There was minimal damage to the structure observed from the exterior. There was no apparent basement for the building. On the east side of the building, there is access to a sub-ground level electrical panel. An elevator is also present on the east side of the building. The estimated distance from ground level to the slab was 0.94 m based on access to the electrical panel room.

Lidar scans were performed at the four corners of the building. The scan numbers for this building are 284, 286, 288, 291, 294. An initial ground reference plane was fit to the site with a 1^{o} slope from the rear (north) to front (south) of the building. Vertical ground displacements relative to this reference plane are shown in Figure 3.3 with a view from the SW corner (Figure 3.3a) and the NE corner (Figure 3.3b) of the building. The lidar scans were also used to estimate building settlements, which are summarized in Figure 3.4. Figure 3.4 also shows the hand-survey laser-level-measured settlements, which are relative to a single datum; however, there were challenges in tying the settlement measurements at the four corners of the building into a single datum. Thus, the lidar-scan measurements are judged to be more reliable. The average building settlement is 40 cm as estimated by the lidar data.

(a)

(b)

Figure 3.2 İskenderun, Hatay. (a) (36.5900N, 36.1772E; 28MAR2023) building surveyed at Apt. No. 34 Ersoz on Bahçeli Sahil Evler Street, and (b) (36.59031N, 36.1771E; 27MAR2023) measurement performed on northeast building corner and showing ground deformation.

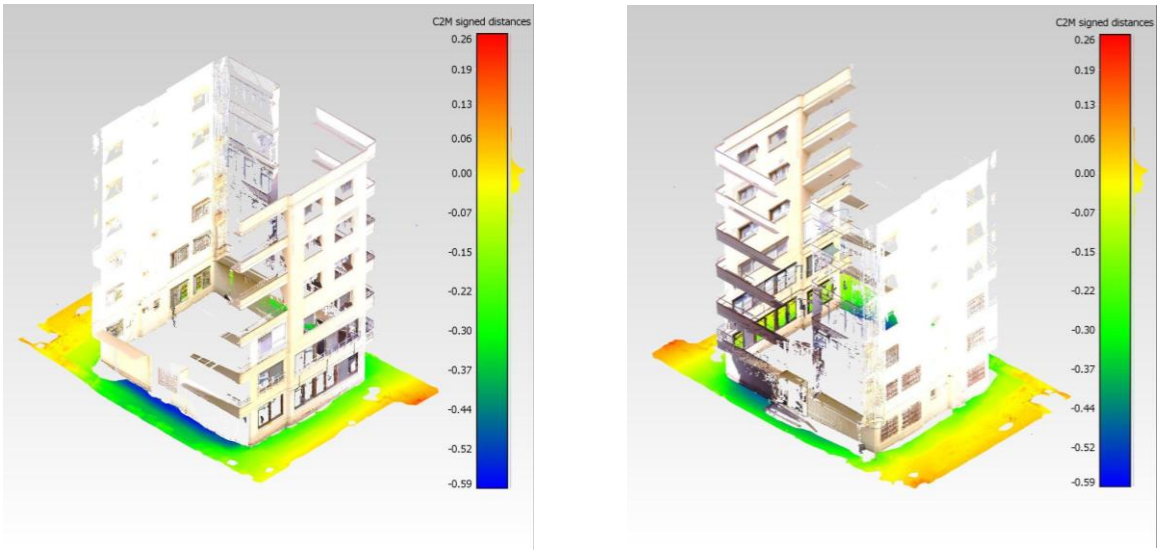

(a) (b)

Figure 3.3. Lidar data from scans no. 284, 286, 288, 291, and 294 of Apt. No. 34 Ersoz showing ground settlement relative to a reference plane that dips 1° from the rear to the front of the building. The color scale on the pictures represents the ground settlement in meters relative to the site reference plane. (a) view of the southwest corner, and (b) view of the northeast corner.

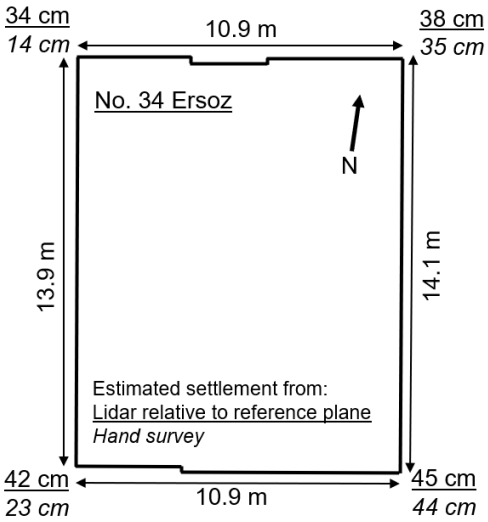

Figure 3.4. Dimensions of the footprint of Apt. No. 34 Ersoz in the Çay district, and the estimated building settlements at each building corner. Settlements were estimated from lidar scans (top #) and hand surveys with laser level (bottom #).

(b. Çay) No. 32 Yenerer, Bahçeli Sahil Evler Street

The residential apartment building No. 32, Yenerer located on Bahçeli Sahil Evler Street (36.5902N, 36.1774E) was surveyed by the GEER Phase 3 team on March 27, 2023. A street-view

picture of the building is shown in Figure 3.5. It is a 5-story building, approximately 15.75 m high. No basement or sublevel was apparent.

Three lidar scans were performed at the building (no. 295, 296, and 298). In addition, scan numbers 286, 288, and 291 from No. 34 captured the ground or structure at No. 32 and were also used. Building settlements were estimated with lidar data relative to an estimated initial reference plane that dips 0.40^{o} from the rear of the lot (north side) to the front of the lot (south side); this reference plane was fit to ground elevations at the site. The ground contours relative to the reference plane and building scan are shown in Figure 3.6. Figure 3.7 shows the building dimensions and estimated settlements from lidar scans and hand surveys. Note that hand-survey laser-level measurements of building settlement were difficult to implement at this building due to uneven settlement of the surrounding ground, and therefore are only provided for one building corner. Based on lidar data, the average building settlement is 50 cm.

(a) (b) (c)

Figure 3.5. (a) (36.5898N, 36.1769E; 28MAR2023) Apt No. 32 Yenerer in Çay district, İskenderun, (b) (36.5901N, 36.1772E; 27MAR2023) view from the southwest corner showng laser level device used to make hand-survey measurements, (c) (36.5903N 36.1774E; 27MAR2023) hand survey at the northeast building corner.

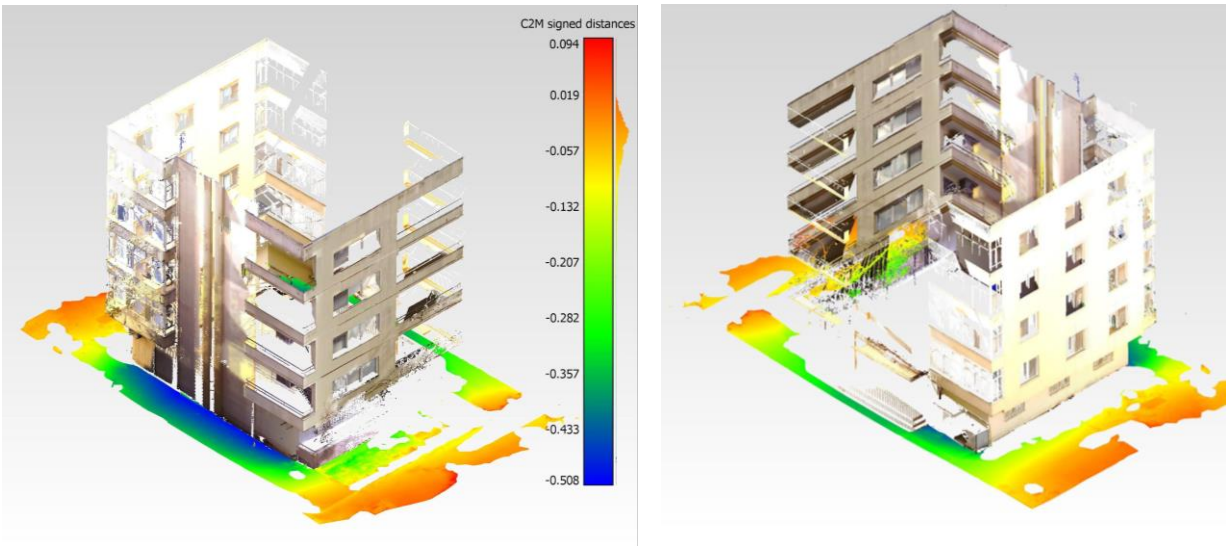

(a) (b)

Figure 3.6. Lidar scan data (from scans no. 295, 296, 298, 286, 288, and 291) showing ground deformations relative to an estimated pre-earthquake reference plane from lidar scans at Apt. No. 32 Yenerer. The color scale on the pictures represents the ground settlement in meters relative to the site reference plane. (a) view of the southwest corner, (b) view of the northeast corner.

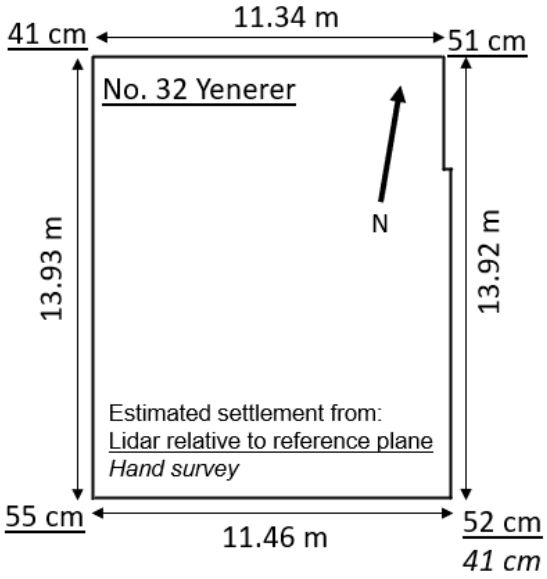

Figure 3.7. Dimensions and building settlement, estimated from LiDAR scans at Apt. No. 32 Yenerer.

(c. Çay) No. 30 UYGAR A.P., Bahçeli Sahil Evler Street

The Apartment No. 30 UYGAR A.P. (36.5902N, 36.1776E) is located on Bahçeli Sahil Evler Street in the Çay district. The street view of the building is shown in Figure 3.8a. The building is 5 full stories with a 6th half story; the height to the top of the 5th floor is approximately 15.65 m.

The owner of the adjacent building (Apt. No. 28), named Ahmet Palalıoğlu, reported that the building has a 3 m deep half-basement. A basement full of water was observed on the west side of the building on March 29, 2023. No basement windows were observed on the east side of the building. Mr. Palalıoğlu also noted that soil sloughing occurred during excavation for the building, which was mitigated with a sheet pile retaining wall. Some cracking on the building exterior was observed to the south side of the building, as shown in Figures 3.8b,c.

Building settlement at the building corners and the building dimensions were obtained from hand surveys with a laser level; these estimates are summarized in Figure 3.9. The building settlement is estimated to be 11 cm, 23 cm, 48 cm, and 43 cm at the northwest, northeast, southeast, and southwest corners, respectively. These settlements are relative to a reference point at the southeast corner of the property, shown in Figure 3.8b. The settlement of 11 cm at the northwest corner of the building is judged to be less reliable because it was difficult to tie-in the laser-level vertical measurement at the northwest corner of the building with the reference point at the southwest corner of the property. Note that these measurements are not corrected for any initial grade of the ground.

(a)

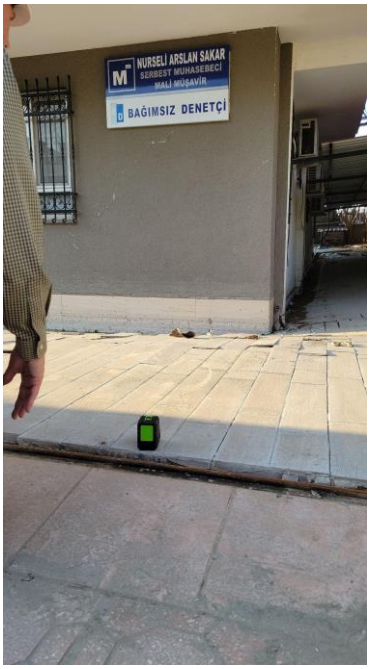

(b)

(c)

Figure 3.8. Surveyed building in the Çay district, Apt. No. 30 UYGAR A.P. (a) (36.5900N, 36.1776E; 28MAR2023), (b) (36.5901N, 36.1776E; 27MAR2023) view of the southeast corner of the building, and (c) southside of the building (36.5901N, 36.1774E; 29MAR2023).

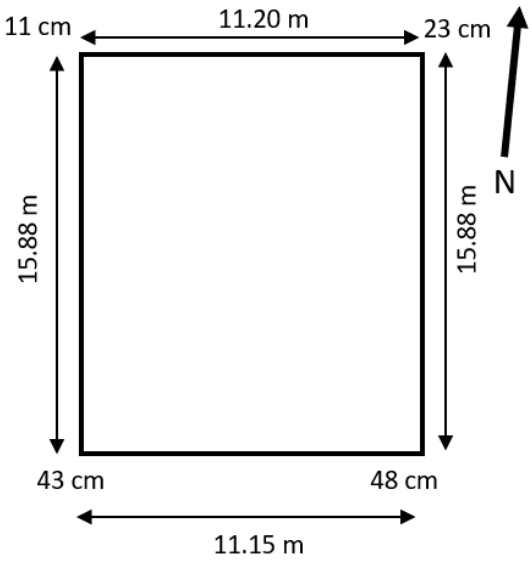

Figure 3.9. Schematic of hand survey measurements of building settlement using a laser level device at Apt. No. 30. Northwest building settlement estimate is less reliable than other measurements.

(d. Çay) No. 28, Bahçeli Sahil Evler Street

The No. 28 apartment building on Bahçeli Sahil Evler Street (36.5902N, 36.1777E) is a 6-story residential building, approximately 19.9 m high. The street view of the building is shown in Figure 3.10a. The building owner, Ahmet Palalıoğlu, reported that the building has a full, 2.8 m deep basement with a 40 cm thick reinforced concrete foundation and the foundation laterally extended 1.5 m around the footprint of the building. Mr. Palalıoğlu also reported that building construction was completed in 2016. Mr. Palalıoğlu reported that regular flooding was occurring in the neighborhood after the 2023 earthquakes. Consequently, he was pumping water from the basement and sealing off the windows to the basement while the GEER Phase 3 team was surveying the building on March 29, 2023. Notable building settlement occurred at this site; the ground deformation pattern is visually evident from the ground pavers in Figure 3.10b.

The building settlements were estimated from lidar scans. One lidar scan was performed at the southwest corner of the building (no. 300) and two scans were performed at the southeast corner (no. 302 and no. 304). An additional scan (no. 303) was performed at the northeast corner, however, it requires additional processing and is not included in the presented survey. The building dimensions and lidar scan data are summarized in Figure 3.11. Building settlements were estimated at the two south corners of the building to be 75 cm and 72 cm for the southwest and southeast corners, respectively. Note that these settlements are relative to a reference point on the ground near the property fence, and are not corrected for any initial grade, although Mr. Palalıoğlu confirmed that the ground did originally slope away from the building. The pattern of ground deformation around the building is shown by the lidar ground contours in Figure 3.11b; these

ground contours summarize the ground settlement below the assumed initial ground level. The ground deformation pattern appears to be consistent with the foundation extending around the building footprint.

(a) (b)

Figure 3.10. Apt. No. 28 on Bahçeli Sahil Evler Street in Çay district, İskenderun, and (b) (36.5900N, 36.1777E) showing ground settlement from the south-west corner of the building.

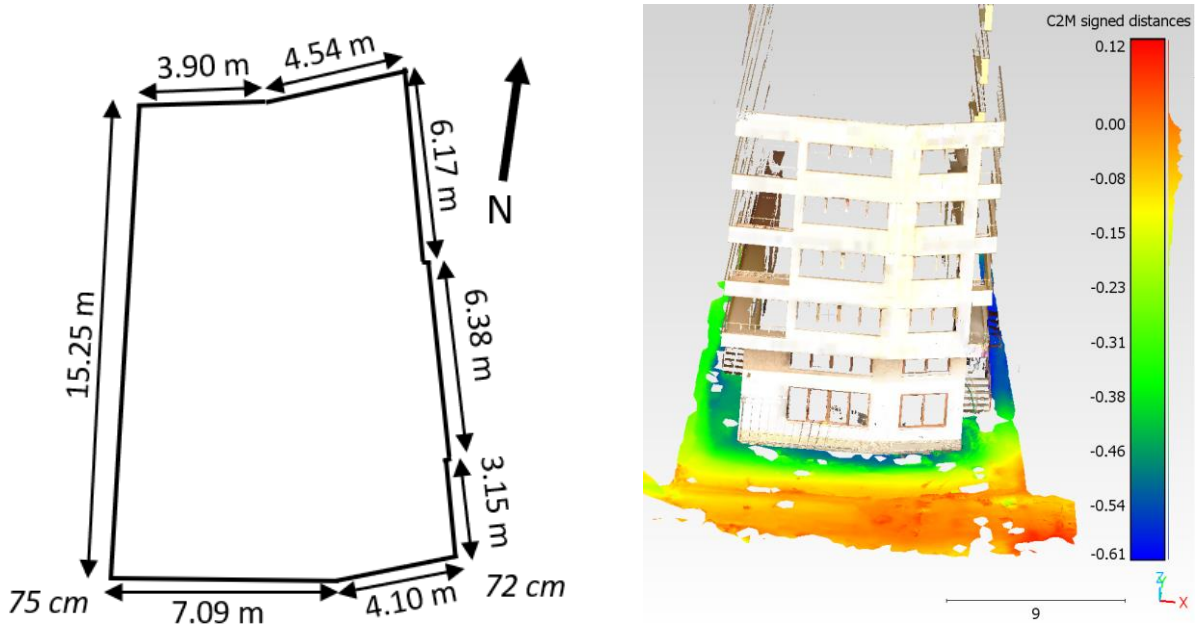

(a) (b)

Figure 3.11. Apt. No. 28 on Bahçeli Sahil Evler Street. (a) settlements and dimensions estimated from lidar scans, and (b) ground deformations from lidar scan data (scans 302, 303, and 304); the color scale on the picture represents the ground settlement in meters relative to the assumed site reference level.

(e. Çay) No. 24, Kaan Ela, Bahçeli Sahil Evler Street

The No. 24 building (36.5903N, 36.1781E) of Bahçeli Sahil Evler Street is a 5-story building approximately 16.5 m high. A street view of the building is shown in Figure 3.12a, note that this picture also shows rolled curbs in front of the building indicating liquefaction in the area. The building owner reported that the foundation has concrete piles beneath a 1-story basement. There was no discernable damage to the structure observed from the outside.

(a)

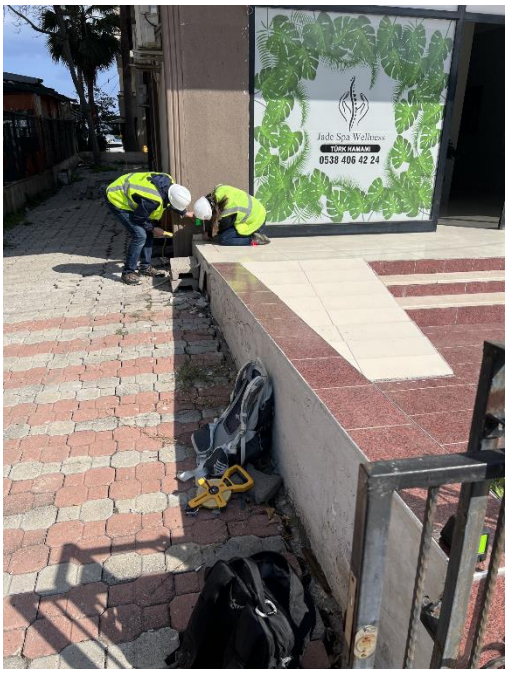

(b)

(c)

Figure 3.12. (a) (36.5900N, 36.1782E; 29MAR2023) street view of Apt. No 24 Kaan Ela, (b) (36.5900N, 36.1777E; 28MAR2023) surveying building settlement at the southwest corner of the building, and (c) (36.5902N, 36.1778E; 29MAR2023) view of the west side of the building and ground.

The average building settlement was estimated as 24 cm based on one lidar scan (no. 306) from the northwest corner of the courtyard. The measured settlements from lidar are estimated from an assumed reference plane that slopes at 0.75^{o} from the rear (north side) of the property to the front. Settlements were also estimated with hand-surveys using a laser-level from the front of the building (Figure 3.12b). The settlements estimated by laser-level survey and lidar scans are summarized in Figure 3.13a; however, it should be noted that the laser-level survey measurements

are not corrected for an initial ground slope. Figure 3.13b shows the building's lidar scan data with a mesh of the ground settlements relative to the assumed reference plane. There was a depression in the ground on the west side of the building (Figure 3.12c) where the ground pavers had fallen into the opening, however it was not apparent what caused this depression. It could potentially be attributed to poor fill compaction near the basement walls leading to excessive settlements and erosion during flooding. The depression was removed from the lidar data in Figure 3.13b since it distorted the scale of the ground settlement adjacent to the building.

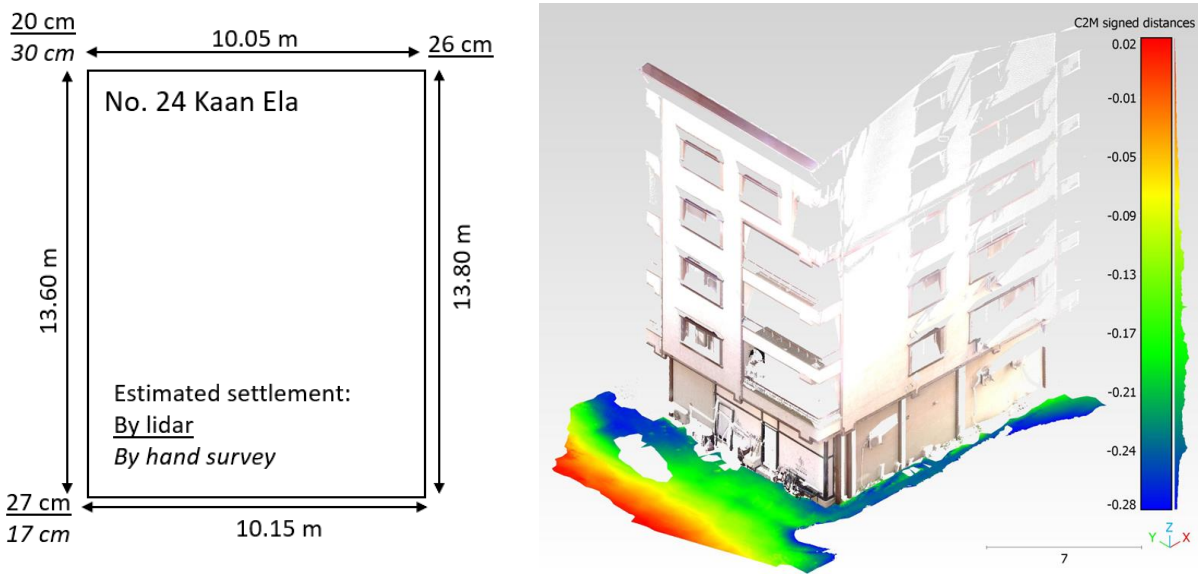

(a) (b)

Figure 3.13. (a) measured dimensions and estimated settlement at Apt. No. 24, (b) lidar scan data (scan no. 306) showing ground settlement relative to an assumed initial slope (reference plane) of the property; the color scale on the figure represents the ground settlement in meters relative to the site reference plane.

(f. Çay) No. 14, No. 16, and No. 18 Kazım Karabekir Street

Liquefaction settlement interactions between buildings were observed for a group of three buildings in the Çay district. The group of three buildings, shown in Figure 3.14a, were two 5-story buildings on either side of a steel-framed single-story restaurant called "Pallet Hookah" (36.5906N, 36.1778E). The settlement from the two 5-story buildings caused a "hogging" pattern of deformation between the two buildings, which appears as a convex bending of the ground, similar to a hog's back. The hogging appeared to cause the large settlement on either side of the Pallet Hookah building and the smaller settlement in the middle. The hogging deformation of Pallet Hookah is visually apparent in Figure 3.14b by the split in the sign located to the left of the "H". Additionally, tension cracks in the floor running between the front and back of the building were observed (3.14c). Negligible damage to the mid-rise buildings was observed from the exterior. About 2 cm of building settlement was estimated from a hand survey using a laser level to the

front center of Pallet Hookah relative to tiled sidewalk in front of the building. Pallet Hookah was measured to settled by an additional 13 cm at its northeast corner and 51 cm at its northwest corner. Relative to the front center of Pallet Hookah, the northwest corner of the building to the east (No. 18 Belli) settled about 40 cm; and the northeast corner of the building to the west (No. 14) settled about 51 cm. The estimates at Building No. 18 are detailed next. Due to limited access, only one measurement at the front of Building No. 14 was obtained.

(a) (b)

(c)

Figure 3.14 Çay District, İskenderun, Hatay. Photos showing liquefaction settlement building interactions. (a) (36.5907N, 36.1778E; 28MAR2023) The Pallet Hookah building appears to have been affected by settlement of two adjacent buildings, (b) (39.5907N, 36.1778E; 28MAR2023) settlement from the two 5-story buildings resulted in a hogging ground deformation, and (c) (36.5907N, 36.1779E; 28MAR2023) the interior of Pallet Hookah with cracks in the floor slab.

The building to the east of Pallet Hookah, called No. 18 Belli, is a 5-story building approximately 16 m high. A street-view of the building is shown in Figure 3.15a, along with pictures of the ground at the front of the building (Figure 3.15b,c). The measured dimensions of the building are

illustrated in Figure 3.16; note that there is a cantilevered section of the building that extends beyond the south side of the foundation by about 1.5 m. This cantilever section is also shown in Figure 3.15d. The building appears to have a small (partial) basement at its west-side associated with an elevator. The GEER Phase 3 team observed that the basement was full of water on March 29, 2023. The extent of the basement is not known since basement windows were not observed around the entire building.

The building settlement of No. 18 Belli was estimated from hand-surveys using a laser-level and one lidar scan from the northeast corner (scan no. 307). These building settlements are apparent in the ground deformations around the building. Additionally, Figure 3.15c shows the ground slope at the front of the building, indicating that the post-earthquake grade slopes towards the building, whereas it is typical for the ground to be graded to slope away from the structure for drainage. The average building settlement, based on the lidar scans, for settlements at the northwest, northeast, and southeast corners is 38 cm.

(a)

(b)

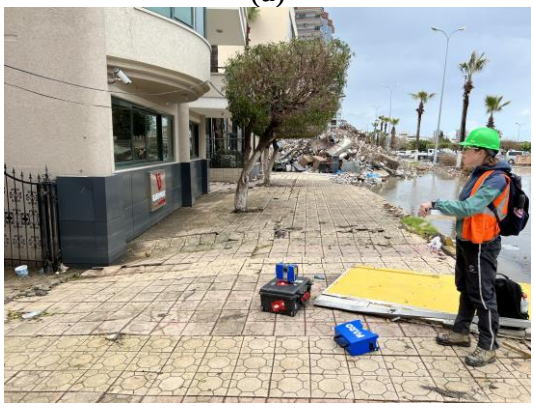

(c)

(d)

Figure 3.15. Building No. 18 Belli: (a) (36.5908N, 36.1779E; 29MAR2023) street view of Building No. 18 Belli (b) (36.5907N, 36.1780E; 29MAR2023) view of the ground from the northwest corner including a view of the cantilever south section, and (c) (36.5907N, 36.1780E; 29MAR2023) view of the ground at the front (north) of the building showing ground deformations that extend around the structure.

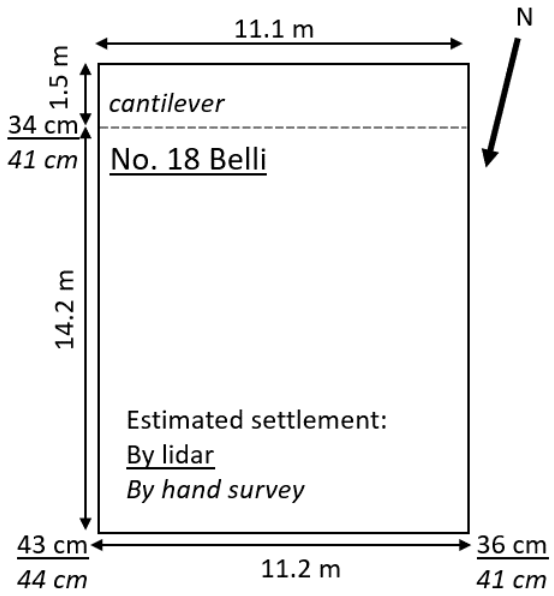

Figure 3.16. Schematic of measured dimensions and settlements at the No. 18 Belli building.

(g. Çay) Four buildings in Çay, İskenderun, Hatay: Apt. No. 26 and 28 Atatürk Boulevard, Apt. No. 14 and 16 Bahçeli Sahil Evler Street.

A group of four buildings was surveyed in the Çay district to document building settlements and the effect on ground deformations around the buildings. The four surveyed buildings were No. 26 Atatürk Boulevard (36.5907N, 36.1789E), No. 28 Atatürk Boulevard (36.5908N, 36.1791E), No. 16 Bahçeli Sahil Evler Street, (36.5905N, 36.1790E), and No. 14 Bahçeli Sahil Evler Street, (36.5906N, 36.1792E). A street-view of the four buildings are shown in Figure 3.17a,b. Figures 3.18a,b show the rear courtyard of the four buildings and the ground deformation induced between them. A hogging deformation pattern was evident based on the convex ground shape and east-west tension cracks through the courtyard tiles. Additionally, on March 29, 2023, flooding in the Çay district inundated the perimeter of the four buildings but the flooding did not inundate the center of the courtyard. Building No. 28 and Building No. 14 appeared to be of similar design and construction and are 6-stories tall with a 7th half-story. Building No. 26 and Building No. 16 also appeared to be of similar design and construction and are 6-stories with a half 7th-story.

(a) (b)

Figure 3.17. (a) (36.5910N, 36.1789E; 1APR2023) Street view of No. 26 and No. 28 in the group of 4 buildings. (b) (36.5903N, 36.1789E; 28MAR2023) Street view of No. 14 and No. 16 in the group of 4 buildings.

The settlements for each building were estimated from (i) lidar scans on March 29 and April 1, 2023 (scan no. 308, 316, 317, 318, and 319), (ii) a laser-level hand-survey survey on April 1, 2023, and (iii) flood water depths on March 29, 2023. The difference of ground levels relative to the reference ground level in the middle of the hogging deformation is shown in Figure 3.19a, along with measured dimensions for the building group. If neither laser-level nor lidar scan estimates were available, the settlement was estimated from measured floodwater depths relative to a lidar scan-based value for the building. Figure 3.19b shows the ground deformations from lidar scan data with the estimated building settlements included as annotation. The lidar data of the ground between the buildings shows the hogging pattern. Building settlements were largest at Building No. 16 (average 65 cm) and Building No. 26 (average 60 cm), and smallest at Building No. 14 (43 cm) and Building No. 28 (34 cm). These estimated settlements do not account for initial surface grades.

(a) (b)

(c)

Figure 3.18 A group of four mid-rise buildings in the Çay district. The photos show hogging ground deformations in the rear courtyard between the four buildings. (a) (36.5907N, 36.1793E; 29MAR2023) rear of south buildings, (b) (36.5907N, 36.1793E; 29MAR2023) rear of north buildings, and (c) (36.5906N, 36.1788E; 29MAR2023) all buildings.

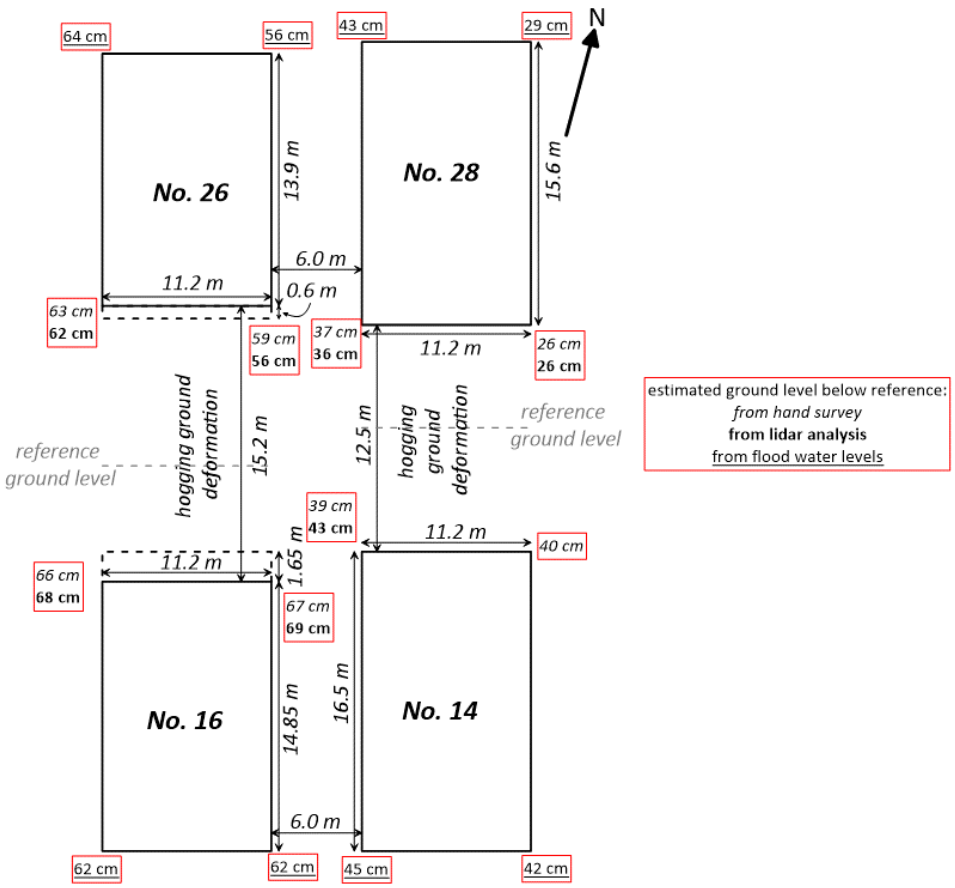

(a)

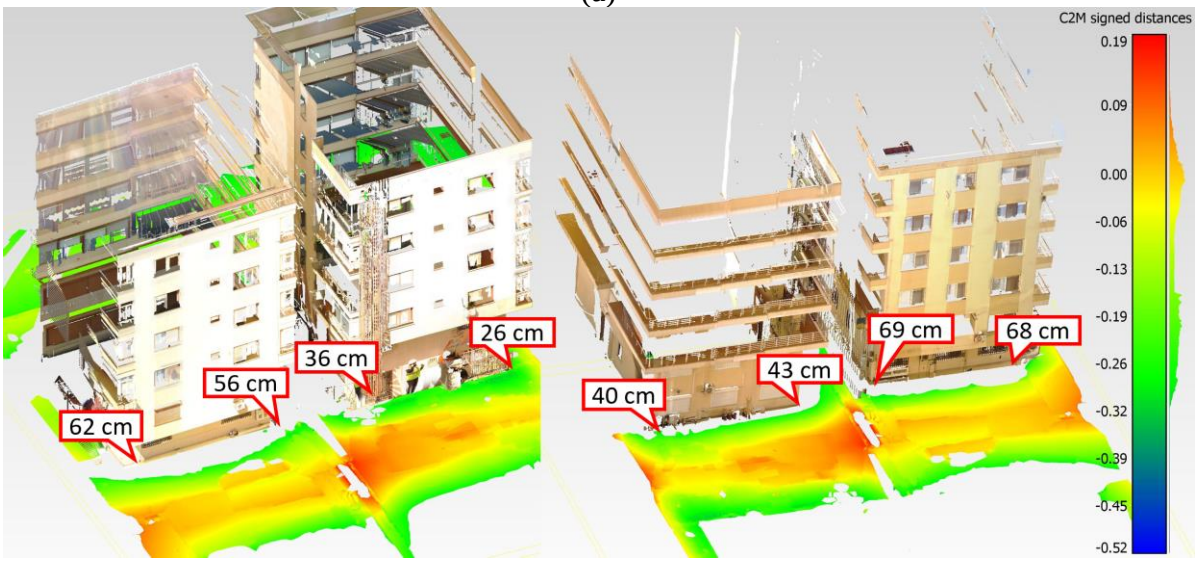

(b)

Figure 3.19 Group of four buildings. (a) summary of measurements and dimensions estimated from lidar scans and hand-survey measurements, and (b) lidar data (from scans 308, 316, 317, 318, and 319) including the pattern of ground deformation for Buildings No. 26 and No. 28 (left) and Buildings No. 16 and No. 14 (right).

3.1.2 Central İskenderun

Building surveys were conducted at nine buildings in central İskenderun. The locations of these surveys are shown in Figure 3.20, with the numbers in the figure representing the building address numbers. These surveys were performed with hand measurements using laser levels. The buildings surveyed had settlements from negligible to over 50 cm. Hogging ground deformation was observed from building settlement around the İskenderun Kindergarten. Sagging ground deformations were observed at adjacent buildings No. 51, 53, and 55 Atatürk Boulevard. One of the buildings briefly surveyed was the civil registry building, also shown in Figures 2.2 and 2.3.

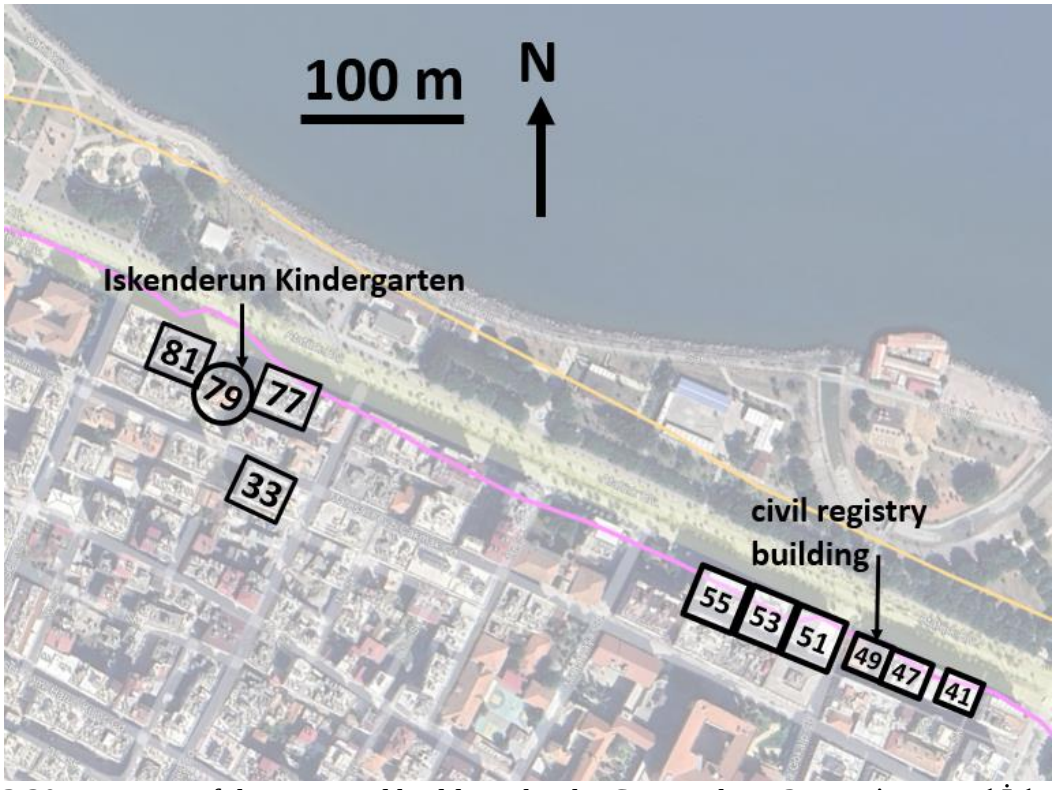

Figure 3.20. Location of the surveyed buildings by the GEER Phase 3 team in central İskenderun. Approximate location of the middle of the figure is 36.5923N, 36.1674E; base image from Google Earth© dated February 16, 2023. The numbers on the figures are the building numbers. Pink line is the approximate 1916 shoreline, orange line is the approximate 1928 shoreline.

(a. İskenderun) Three buildings in İskenderun: No. 41, No. 47, and No. 49 Atatürk Boulevard

Rapid building settlement surveys were performed at three row buildings in the same block on Atatürk Boulevard: No. 41, No. 47, and No. 49. Building No. 49 is the civil registry building (Figure 2.3) that was originally built along the pre-1916 shoreline. Settlement at all these buildings was estimated at a point in the middle of the building front and relative to a point on the sidewalk that was considered to have not settled. The survey at Buildings No. 49 and 47 shared a reference point. Building No. 41 is a 6-story building with apparent mixed commercial and residential use. Approximately 16 cm of settlement was measured at Building No. 41. There

was some standing floodwater present at Building No. 41 as shown in Figure 3.21.

Figure 3.21. (36.5914N, 36.1710E; 28MAR2023) Building settlement survey and standing floodwater at No. 41 Atatürk Boulevard.

The measured building settlement at No. 47 and No. 49 was 13 cm and 7 cm, respectively. Consequently, there was approximately 6 cm of settlement difference between the two buildings. The two buildings are pictured in Figure 3.22a where No. 47 is in the background and No. 49 is in the foreground. Standing floodwater was present when the buildings were surveyed on March 28, 2023; however, there was notably less water in front of Building No. 49 as shown in Figure 3.22a. Figure 3.22b shows the shared sides of the buildings; there were no apparent interactions between the two structures. Figure 3.22c shows the standing floodwater in the alley on the east side of Building No. 47. The presence of floodwater is notable at these structures and suggests that there may have been widespread ground settlement in addition to the surveyed settlement at individual buildings.

(a)

(b)

(c)

Figure 3.22. Surveys at Buildings No. 47 and No. 49 Atatürk Boulevard. (a) (36.5918N, 36.1703E; 28MAR2023) both buildings with standing floodwater in front of No. 47, (b) (36.5918N, 36.1703E; 28MAR2023) side-by-side view, and (c) (36.5915N, 36.1705E; 28MAR2023) standing floodwater in the alleyway east of Building No. 47.

(b. İskenderun) Three buildings in İskenderun: No. 51 (Deniz Bank), No. 53, No. 55 Atatürk Boulevard

A row of three commercial buildings along Atatürk Boulevard was characterized by hand survey. The addresses are No. 51, No. 53, and No. 55 Atatürk Boulevard (36.5918N, 36.1690E). Photos of the buildings are shown in Figure 3.23, and a schematic of dimensions and settlement in Figure 3.24. The east building is a bank building and approximately 16.2 m high; it appeared to have very little building settlement, and some fill settlement was observed around the east side of the building as shown in Figure 3.23d. The settlements at this building ranged from 0 cm at the east side to 21 cm at the west side. The middle building is approximately 15.2 m high. The measured building settlements ranged from 21 cm at the east edge to 38 cm at the west edge. The west building is approximately 21.6 m high; its settlements ranged from approximately 41 cm at the east edge to 32 cm at the west edge. The settlements of these three buildings indicates a “sagging” ground deformation pattern along this building row. This sagging interpretation was additionally

supported by the presence of standing water on April 1, 2023 (when the buildings were surveyed) that was primarily located around the middle building (see Figure 3.23c).

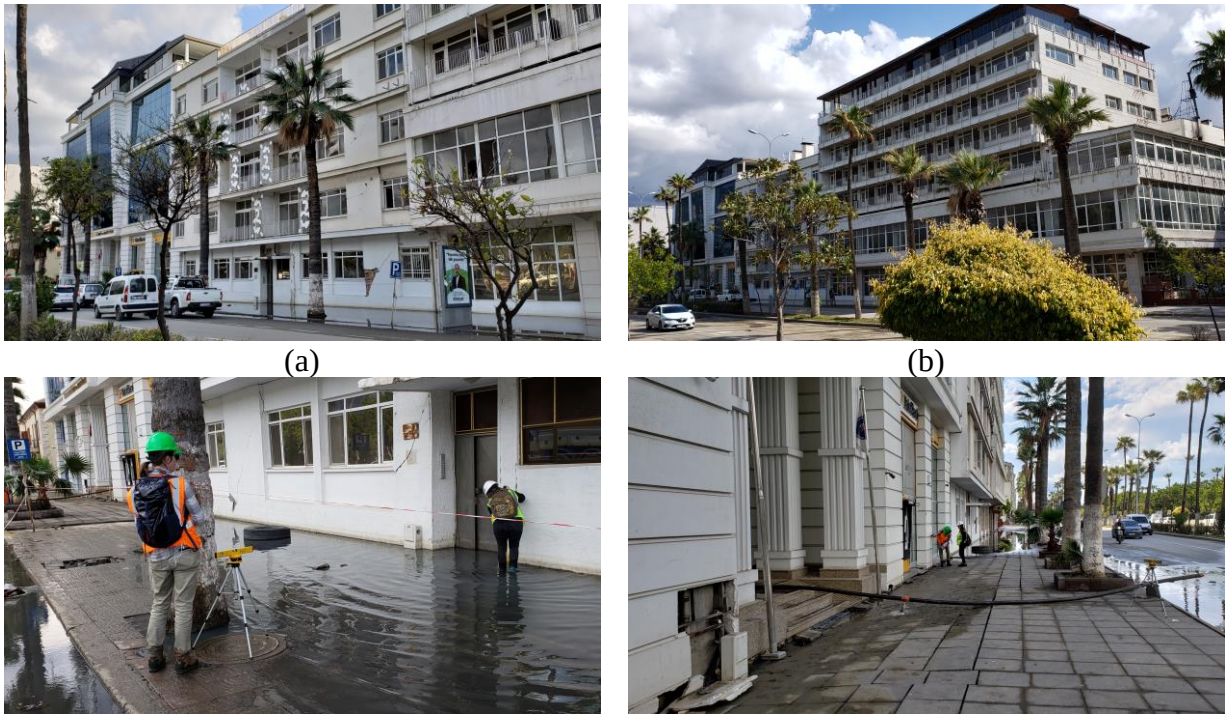

(a) (b) (c) (d)

Figure 3.23. Hand surveys of buildings No. 51, No. 53, and No. 55 Atatürk Boulevard: (a) (36.5920N, 36.1694E; 1APR2023), (b) (36.5924N, 36.1689E; 1APR2023), (c) (36.5924N, 36.1689E; 1APR2023), and (d) (36.5916N, 36.1670E; 1APR2023)

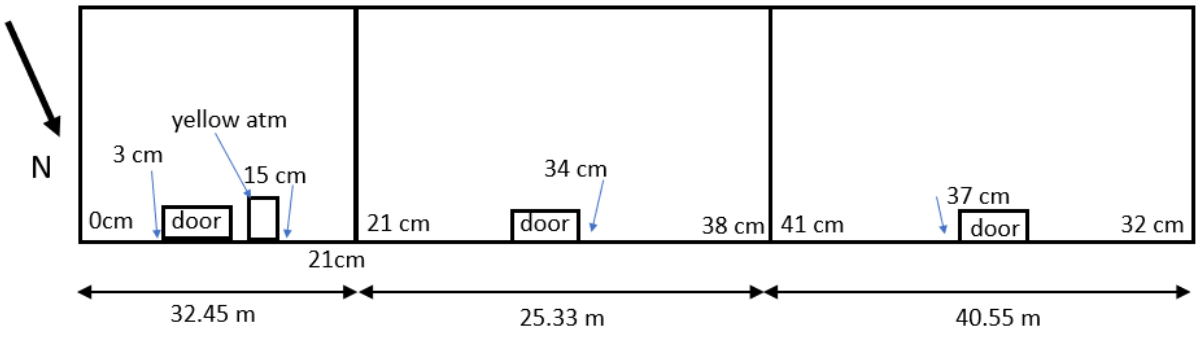

Figure 3.24. Schematic of measured building settlements and dimensions at the row buildings along Atatürk Boulevard.

(c. İskenderun) Three buildings in İskenderun: No. 77, No. 79 (İskenderun Anakoulu/İskenderun Kindergarten), and No. 81 Atatürk Boulevard

The influence of building settlement on ground deformation was observed for a group of three buildings in İskenderun. The three buildings include two commercial buildings (No. 77 and No.

81) located on Atatürk Boulevard, and a kindergarten (No. 79 İskenderun Anakoulu) set back approximately 21 m from Atatürk Boulevard (36.5930N, 36.1676E). A street view photo of the kindergarten is shown in Figure 3.25, which also shows the hogging ground deformation on the sidewalk in front of the kindergarten. The manager of the kindergarten reported that the building settled a small amount, however, no discernible settlement was observed by the GEER Phase 3 team. The GEER team measured a length of about 9 m on the sidewalk in front of the kindergarten that was not impacted by settlement of the adjacent commercial buildings. This suggests the hogging pattern may have leveled out near the center of the kindergarten.

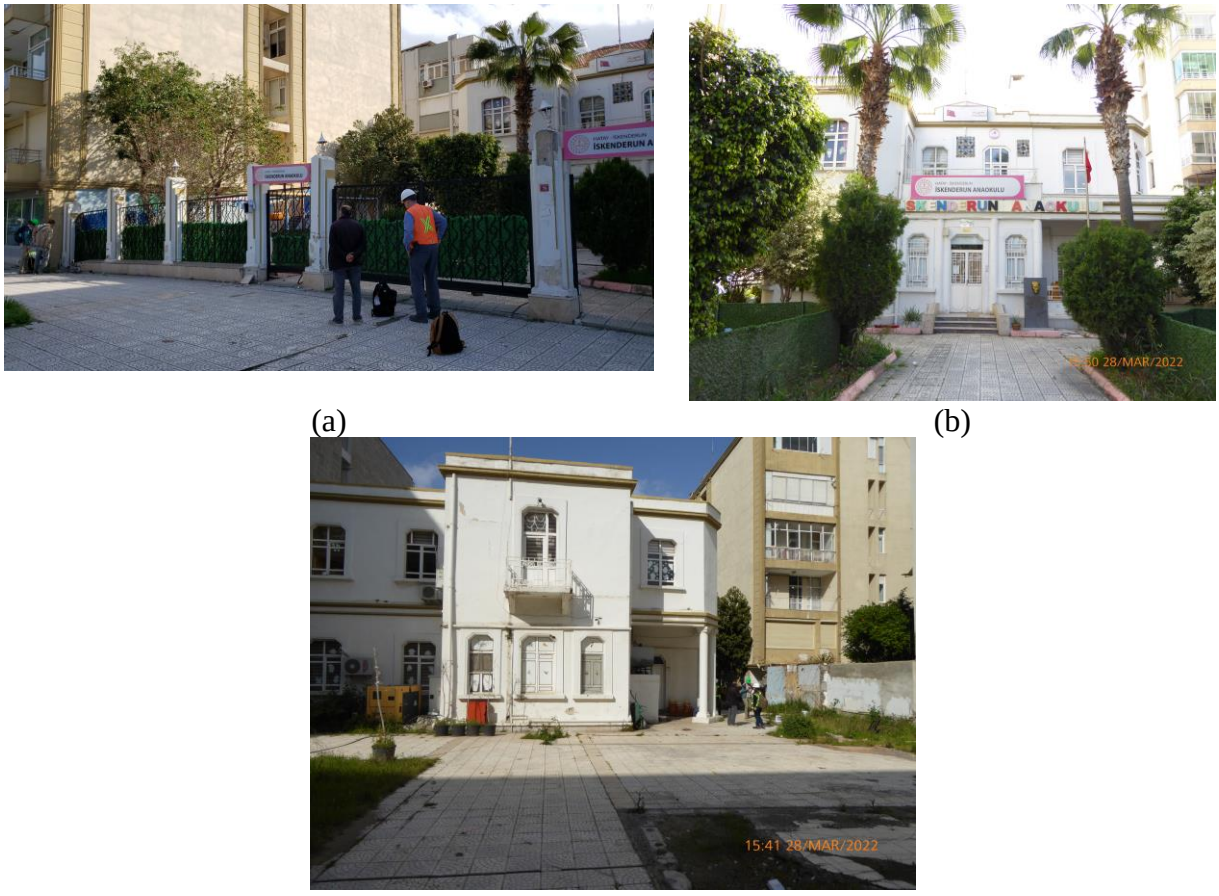

(a) (b)

(c)

Figure 3.25 The kindergarten (İskenderun Anakoulu) showing hogging ground deformations from the adjacent buildings. (a) (36.5933N, 36.1659E; 28MAR2023) sidewalk in front of the kindergarten with hogging deformation, (b) (36.5933N, 36.1658E; 28MAR2023) front view of the kindergarten, and (c) (36.5931N, 36.1656E; 28MAR2023) rear view of the kindergarten.

(a) (b) (c)

Figure 3.26 Buildings adjacent to the kindergarten. (a) (36.5928N, 36.1661E; 28MAR2023) building to the east of the kindergarten (No. 77), (b) (36.5934N, 36.1657E; 28MAR2023) building to the west of the kindergarten (No. 81), and (c) (36.5934N, 36.1657E; 28MAR2023) building to the west of the kindergarten.

The hogging ground deformation is attributed to settlement of the two relatively tall commercial buildings on either side of the kindergarten, shown in Figure 3.26. The settlement of the two buildings was measured by laser-level from a point on the sidewalk in front of the kindergarten gate that did not appear to settle. The measured settlements are summarized with a schematic drawing in Figure 3.27. The building to the east (No. 77) is a 6-story building; the manager of the kindergarten reported that this building does not have a basement. The measured settlement at the front of No. 77 was 42 and 47 cm for the northeast and northwest corners, respectively. The building to the west of the kindergarten (No. 81) is a 6-story building; the manager of the kindergarten reported that this building has a basement. The measured settlement was 45 and 55 cm for the northeast and northwest corners, respectively.

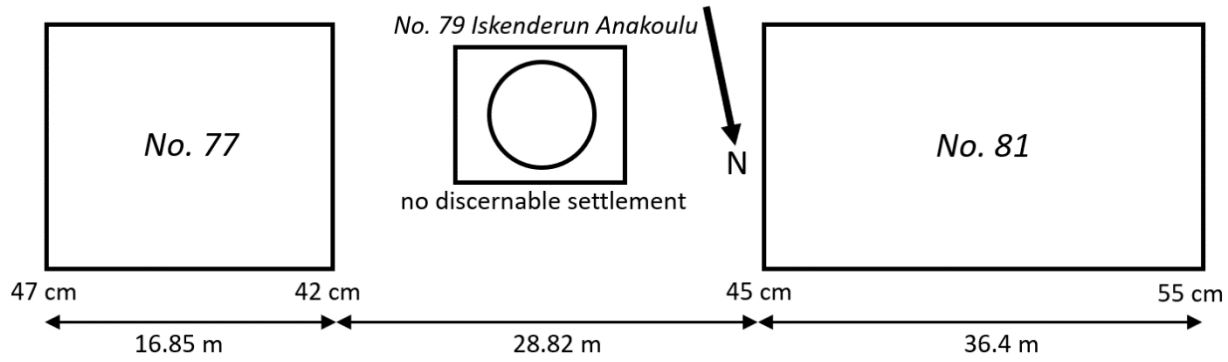

Figure 3.27. Schematic of measured building settlements and dimensions of the buildings adjacent to the İskenderun Anakoulu.

(d. İskenderun) No. 33 Mareşal Fevzi Çakmak Street

The team surveyed Building No. 33 Mareşal Fevzi Çakmak Street on March 28, 2023. This building underwent less than 10 cm of settlement in an area where larger settlements were observed. The 5-story residential row building has first floor commercial use and faces northeast (Figure 3.28). The adjacent lot northwest of the building is empty; a building to the southeast is in in contact with the surveyed building. Deformation of the sidewalk adjacent to Building No. 33 indicates that building settlement took place (Figure 3.28b). Surveys of settlement from the sidewalk to the northwest edge, center, and northeast edge of the building measured settlements of 5 cm, 7 cm, and 6 cm, respectively, indicating a slight sag in the center of the building. Figure 3.28c shows the laser-level survey at the center of the building. The front of the building (northeast edge) was measured as 26.55 m in width. The length of the building is approximately 19 m (estimated on Google Earth from the northwest edge). The building is approximately 16.1 m in height. The building owner reported that there is no basement. No exterior damage was observed.

(a)

(b)

(c)

Figure 3.28. Çay district in İskenderun, Hatay building with small settlement: (a) view of building facing west (36.5926N, 36.1662E, 28MAR2023), (b) (36.5926N, 36.1661E, 28MAR2023) deformed sidewalk, and (c) (36.5927N, 36.1661E, 28MAR2023) laser-level survey to the center of the building relative to "stable" sidewalk (dashed green line indicates assumed original ground level).

3.2 Gölbaşı, Adıyaman

The GEER Phase 3 team surveyed buildings in Gölbaşı, Adıyaman province on April 1, 2023. In total, 12 buildings were surveyed with settlements ranging from negligible to over 1 m. The surveyed buildings ranged from 2-story to 6-story buildings. A summary of the buildings surveyed, along with lidar scan locations are shown in Figure 3.29. In-depth surveys were conducted at buildings A and B on Zübeyde Hanim Street, No. 91 Gazi Street, and the apartment complexes constructed by Yarımay Inş and Cihan Inş. Brief surveys were conducted at Buildings No. 88, No. 90A, No. 92, No. 94 Gazi Street and No. 13 52 Sk.

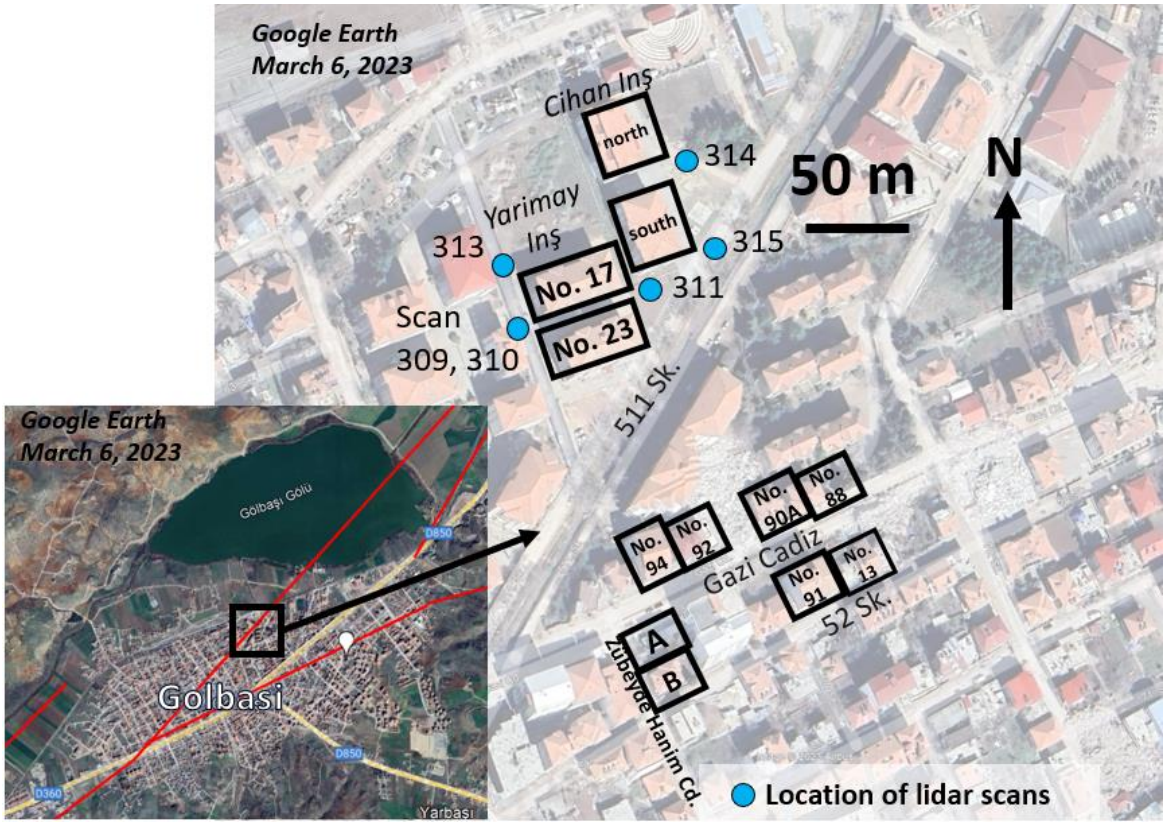

Figure 3.29. Locations of surveyed buildings and lidar scans by GEER Team 3 in Gölbaşı.

(a. Gölbaşı) Two 5-story apartment buildings on 511 Street, No. 17 and No. 23, constructed by Yarımay Construction.

Two adjacent five-story apartment buildings on 511 street in Gölbaşı were observed to document their differences in performance. The apartments were constructed by "Yarımay Inş". The apartment building No. 23 is the north building (Figure 3.30a) and No. 17 is the south building (Figure 3.30b). Both apartment buildings are nearly identical in appearance, with the exception that Building No. 17 has a one-story basement and Building No. 23 has no basement. The structures are composed of a reinforced concrete frame with masonry infilled walls. From Google Earth images, construction at No. 23 was completed after June 2021 and construction at No. 17 was completed after August 2019. They are located within 700 m of the Gölbaşı Lake to the north, and they are adjacent to a channelized creek just across 511 street at the south.

(a) (b)

Figure 3.30. Apartments constructed by Yarımay Inş. (a) (37.7890N, 37.6422E; 30MAR2023) No. 23, the north building, image obtained from lidar scan, (b) (37.7890N, 37.6422E; 30MAR2023) No. 17, the south building, image obtained from lidar scan.

Both buildings did not appear to have structural damage; however, they showed obvious signs of building settlement around their perimeter. Building settlement and ground cracks were observed around No. 17 (the south building) as shown in Figures 3.31a,b,c. The owners allowed access into the building's basement, which was observed to have some ponded water along its southern wall (Figure 3.31d). Although the owners mentioned that water often puddles in the basement due to the lack of a sump pump, the water may also indicate some tilt towards the south. Traces of soil (i.e., possible ejecta) and minor cracking of the concrete floor were also observed near structural columns within the basement.

(a)

(b)

(c)

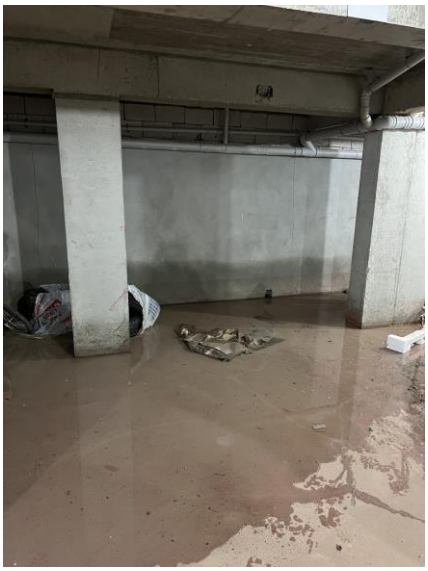

(d)

Figure 3.31. Yarımay İnşaat Apartments No. 17 (south building). (a) (37.7890N, 37.6428E; 30MAR2023) southeast corner of No. 17 showing ground deformation, (b) (37.7891N, 37.6429E; 30MAR2023) northeast corner showing ground settlement, (c) (37.7889N, 37.6428E; 30MAR2023) south view showing ground settlement, and (d) (37.7890N, 37.6427E; 30MAR2023) standing water in the basement of the south building.

No. 23 (the north building) showed significant settlement and separation from the adjacent ground at its southeast corner (Figure 3.32a). Extensional cracking observed along the north and south wall of the building (parallel to the lakeshore) totaled about 45 cm, which approximately matched the accumulated cracking along a nearby concrete wall (perpendicular to the lakeshore) (Figures 3.32b,c).

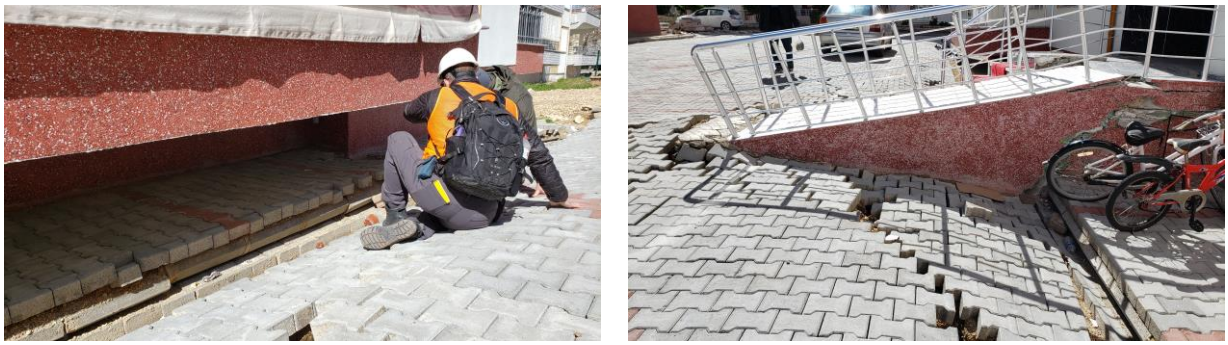

(a) (b)

(c)

Figure 3.32. Yarımay İnşaat Apartments No. 23: (a) (37.7892N, 37.6462E; 30MAR2023) ground settlements near the southeast corner, (b) (37.7892N, 37.6426E; 30MAR2023) ground deformation around the south entrance, and (c) (37.7895N, 37.6426E; 30MAR2023) cracking in a concrete wall that runs approximately north-to-south; the northeast corner of No. 23 is in the background.

Lidar scans were performed for these apartment complexes (i.e., scan numbers 309, 310, 311, and 313) with approximate locations as shown in Figure 3.29. The initial estimates of the building settlements and building dimensions from the lidar scans are shown in Figure 3.33 and Figure 3.34. No. 23 (the north building) is settled considerably more than No. 17 (the south building). The average building settlement at No. 23 is 1.02 m and the average building settlement at No. 17 is 0.22 m.

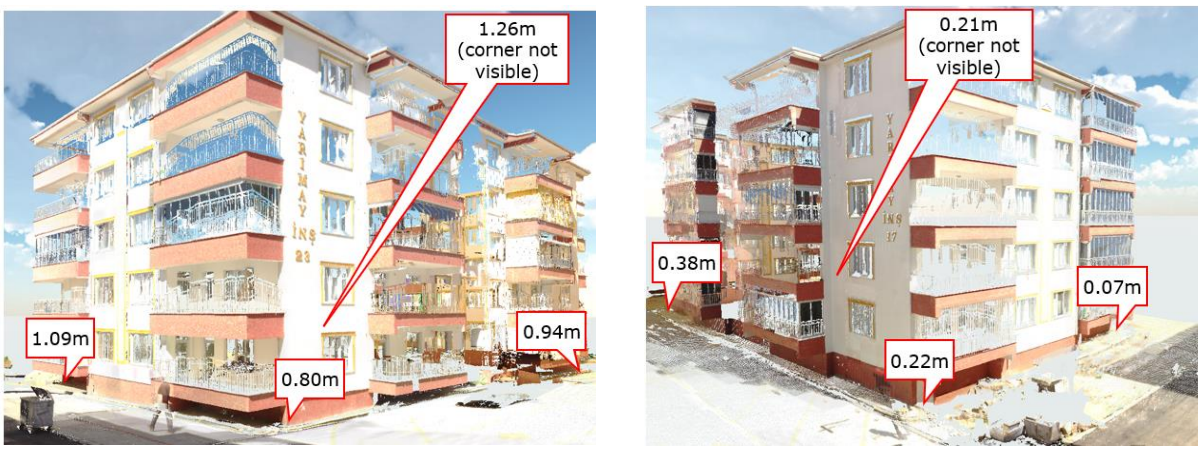

(a) (b)

Figure 3.33. Lidar scan results data with estimated settlements for Yarımay İnşaat Apartments: (a) No. 23, and (b) No. 17.

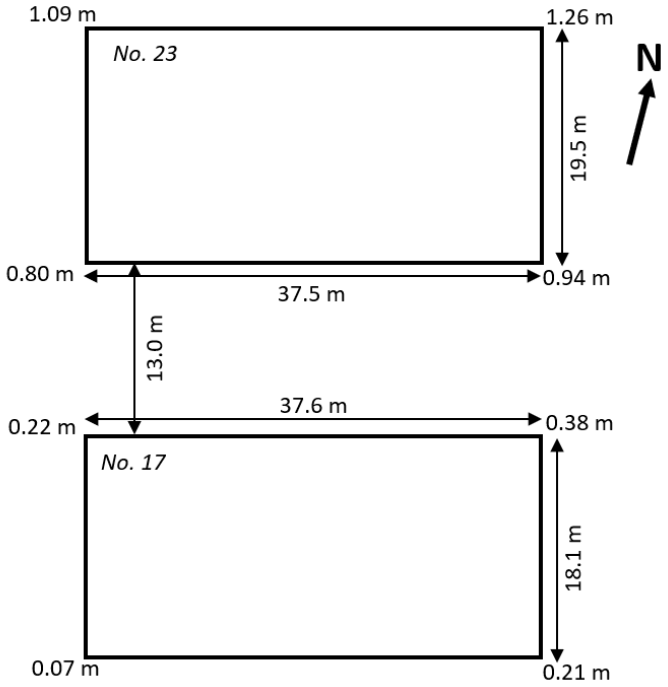

Figure 3.34. Schematic of estimated dimensions and settlements from lidar scans of the two Yarımay İnşaat apartment buildings.

(b. Gölbaşı) Two 5-story apartment buildings on 511 Street, by Cihan Construction

An additional pair of apartment buildings were characterized on 511 Street. The apartment complex was constructed by "Cihan İnşaat". The building numbers are not known by the authors; therefore, the buildings will be referred to as the north building (37.7899N, 37.6427E) and the south building (37.7896N, 37.6429E). The buildings are shown in Figure 3.35. The buildings

appear to have similar design and construction. Images from Google Earth indicate that the buildings were constructed at a similar time with construction starting after June 2017 and appearing to be mostly complete by August 2019. The buildings are similar in appearance and design; however, the north building has a basement, which was 2.9 m high from the top of slab to the bottom of the ceiling. There was no obvious damage to the structures observed from their exterior.

(a)

(b)

(c)

Figure 3.35. Cihan İnşaat apartment complex: (a) the north building (37.7902N, 37.6423E; 30MAR2023), (b) the south building (37.7889N, 37.6427E; 30MAR2023), and (c) north building settlement at along south east side of building (37.7894N, 37.6431E; 30MAR2023),

Two lidar scans on the east side were performed for the buildings (scan no. 314 and 315). These lidar scans allow estimation of settlement at the two east corners of the south building, and settlement at the southeast corner of the north building. The lidar scan data and measured settlements are shown in Figure 3.36. The building settlement and ground damage are shown in Fig. 3.35c. The estimated settlement at the south building is 36 cm and 72 cm for the southeast and northeast corners, respectively. The estimated settlement at the southeast corner of the north building is 3 cm. These settlements are estimated relative to a reference point on the road in front of the south building, which did not appear to have settled.

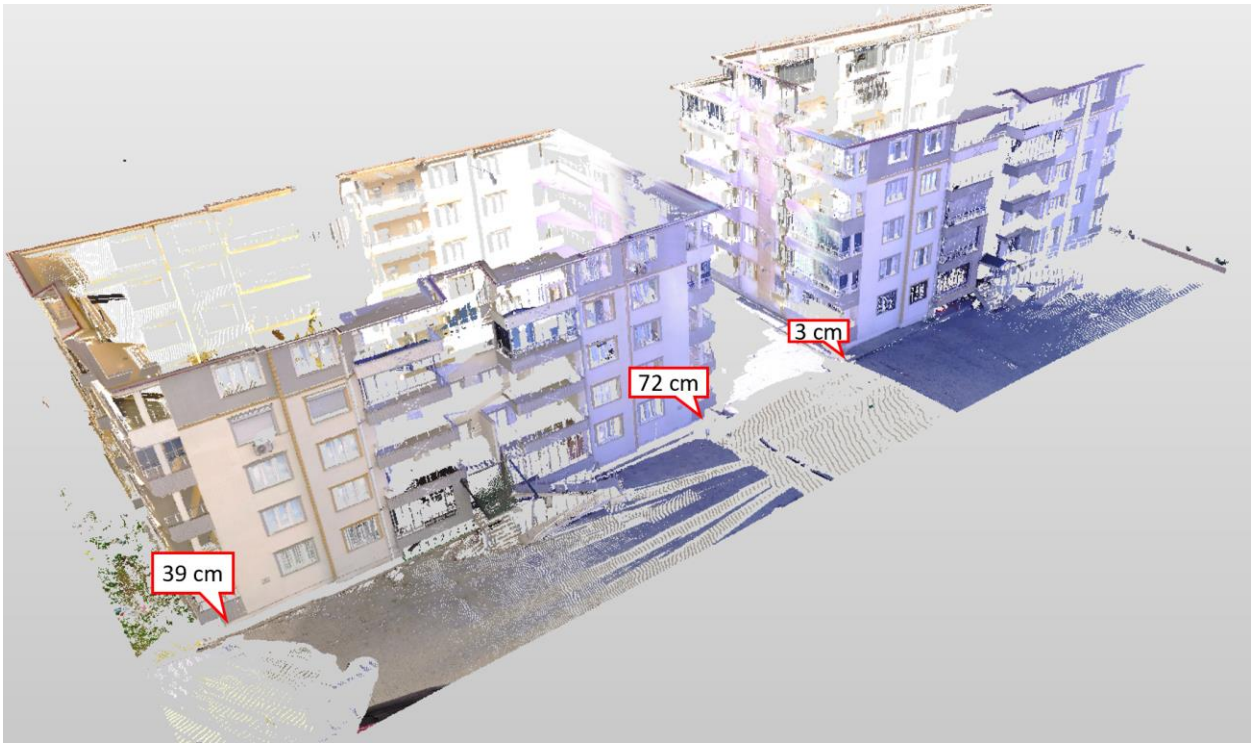

Figure 3.36. Lidar scan data from Cihan İnşaat and estimated settlements from lidar analysis. The north building with a basement is shown at the upper right part of the scan, whereas the south building without a basement is shown in the lower left part of the scan.

(c. Gölbaşı) Two 2-story residential buildings on Zübeyde Hanım Street

Two adjacent two-story residential buildings were surveyed to document their differences in performance. A two-story plaster and cinder single residential building is located on the southeast corner of Zübeyde Hanım Street and Gazi Street (37.7877N, 37.6429E). The second building is a two-story multi-residential building located on the northeast corner of Zübeyde Hanım Street and 52. Sk (37.7876N, 37.6430E). These buildings are documented herein due to the contrasts in their performance. Ejecta was documented in the yard between the two buildings and two soil samples were obtained. These buildings are described in further detail below.

Negligible settlement was observed at the two-story single-residential building (37.7877N, 37.6429E). The building is 10.32 m long north-to-south and 13.4 m wide east-to-west with an additional -m wide garage on the east side (Figure 3.37a). The building is approximately 5.6 m high. From examining Google Earth images, the structure was built after 2019. The structure appears to be cinder block and plaster construction with no apparent basement. Although there was negligible settlement documented, there was damage to the structure that appeared to be due to ground deformation at the structure to the east. Figure 3.37b shows the notable settlement at the east-adjacent structure. An approximately 10 cm crack was observed on the south side of the building near the connection between the house and the garage (Figure 3.37c); additionally, a 1^{o} tilt towards the house was measured on the east wall of the garage.

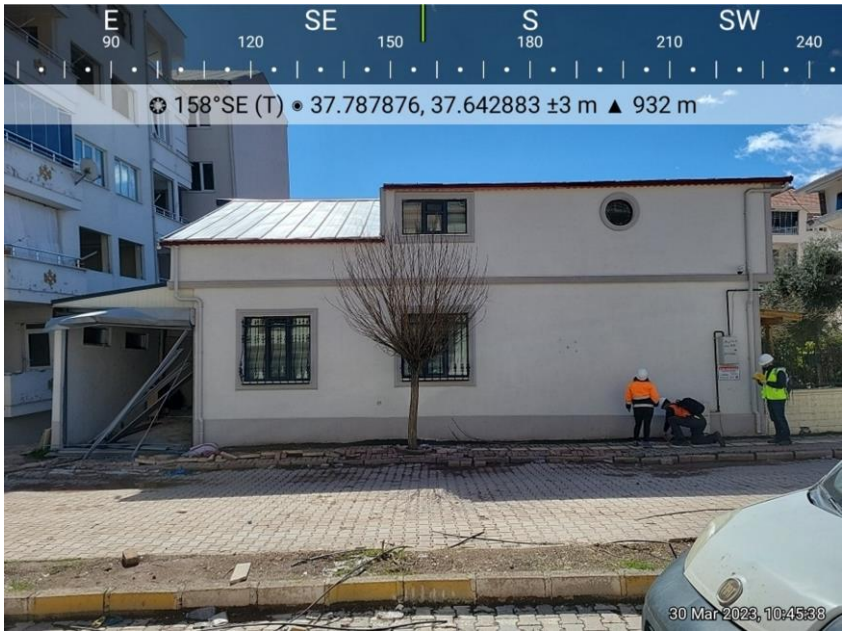

(a)

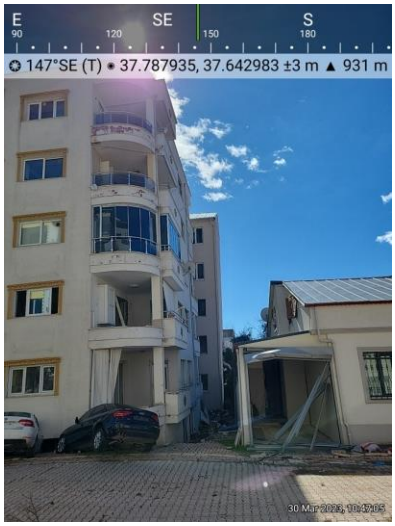

(b)

(c)

Figure 3.37. 2-story cinder block and plaster construction residential building in Gölbaşı with no discernable settlement: (a) (37.7879N, 37.6429E; 30MAR2023) street view of the building with attached garage showing disturbance in the adjacent sidewalk and road, (b) (37.7879N, 37.6430E; 30MAR2023) settlement at adjacent 5-story building and its effect on the attached garage, and (c) (37.7877N, 37.6431E; 30MAR2023) crack that opened on the south side of the house due to displacement of the garage.

Significant building settlement was observed at the two-story building (37.7876N, 37.6430E) as shown in Figures 3.38a-c. The building was measured to be 9.9 m wide north-to-south and 12.2 m long east-to-west with an approximate height of 7 m. From examining Google Earth images, the structure was constructed prior to 2008. Settlement at the front door building entrance at the

southwest corner was measured to be over 1.1 m. Ponded water was present along the south side of the building. The east perimeter of the building settled about 20 cm more than the west perimeter of the building, inducing some tilt. The building owner told our team that the building was originally constructed without the partial shallow storage area, which was later built under the backyard cantilevered patio.

(a) (b)

(c)

Figure 3.38. Settled two-story residential building with a partial basement in Gölbaşı: (a) view of building from southwest corner (37.7874N, 37.6429E; 30MAR2023), (b) collapsed deck over partial shallow storage area along north wall (37.7878N, 37.6429E; 30MAR2023), and (c) front door entrance at southwest corner with over 1.1 m of measured settlement (37.7875N, 37.6430E; 30MAR2023).

(d. Gölbaşı) No. 91 Gazi Street

Settlements at No. 91 Gazi Street (37.7880N, 37.6438E) were surveyed at the north side of the building with hand measurements using a laser-level. The building is a 6-story residential apartment building. Some cracking was observed in the first floor exterior of the building at the front and rear (Figure 3.39). The dimensions were measured as 20.0 m by 16.6 m with an approximate height of 19.4 m. Settlements were measured across the front (north side) of the

building where ground deformations were observed. Ground settlement is captured at the front and rear of the building in Figure 3.40. The settlements and dimensions are summarized in Figure 3.41. At the front of the building, 18 cm was measured at the northeast corner and 22 cm was measured at the northwest corner. There was no measurable tilt on the west side of the building.

(a) (b)

Figure 3.39. Survey at No. 91 Gazi Street. (a) (37.7882N, 37.6437E; 30MAR2023) street view, and (b) (37.7878N, 37.6437E ; 30MAR2023) rear view of the building including cracks in the exterior of the first floor.

(a) (b)

Figure 3.40. Ground deformations around No. 91 Gazi Street. (a) (37.7882N, 37.6438E; 30MAR2023) ground deformations at front of the building, and (b) (37.7880N, 37.6439E; 30MAR2023) ground deformations at the rear of the building.

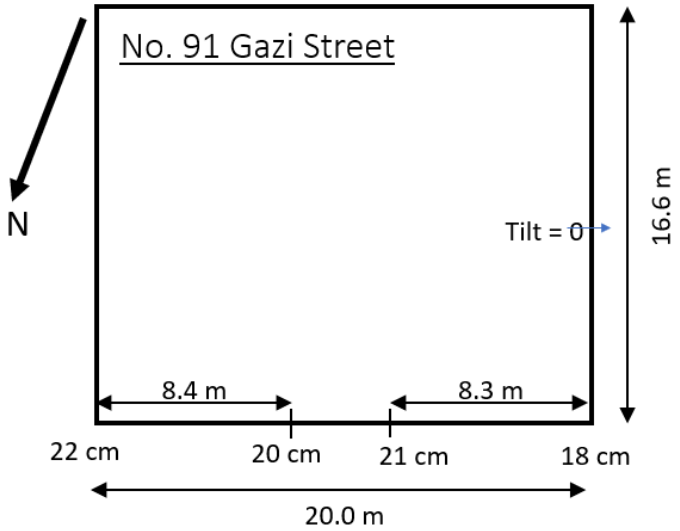

Figure 3.41. Schematic of surveyed settlements and dimensions of No. 91 Gazi Street, including distance between measured settlement points.

(e. Gölbaşı) No. 13 52 Sk.

Building No. 13 52 Sk. (37.7880N, 37.6440E) is a 1-story house. Pictures of the house are shown in Figure 3.42. Based on a hand-survey of measurements on the south and west sides of the structure, there was an average 13 cm of building settlement. A neighbor reported that the foundation is a 50 cm thick mat.

(a) (b)

Figure 3.42. No. 13 52 Sk. (a) (37.7879N, 37.6440E; 30MAR2023) view of the south side, and (b) (37.7879N, 37.6440E; 30MAR2023) view of the westside.

(f. Gölbaşı) No. 88 Gazi Street

Building No. 88 Gazi Street (37.7883N, 37.6438E) is a 4-story residential building. A summary of the estimated settlements, at two points on the south face of the building, the building tilt, and dimensions (measured on Google Earth) are summarized in Figure 3.43. The average building settlement was 54 cm. Tilts of 1^{o} towards the east and 3^{o} towards the south were measured for this building. A building resident reported that the building does not have a basement and has a 1 m-thick mat foundation.

(a)

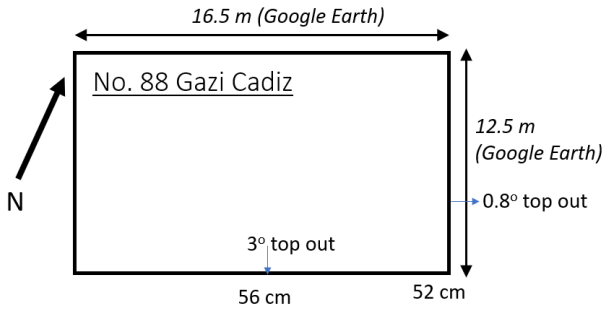

(b)

Figure 3.43. No. 88 Gazi Street: (a) (37.7883N, 37.6440E; 30MAR2023) street view, and (b) schematic illustration of hand-surveyed settlements, tilts, and estimated dimensions.

(g. Gölbaşı) No. 90A Gazi Street

No. 90A Gazi Street (37.7883N, 37.6436E) is a 3-story building with a convenience store on the first level and what appear to be residential units on the second and third floors. A summary of the estimated settlements, at two points on the south face of the building, the building tilt, and dimensions (measured on Google Earth) are summarized in Figure 3.44. The building settlement at the southeast corner was estimated as 1 cm and the building settlement at the southwest corner was estimated as 39 cm, indicating a differential settlement of 38 cm over the length of the building (i.e., a length of 13 m as measured from Google Earth). The measured tilt at the east side of the building was 3° towards the west. The measured tilt at the south side (front) of the building was 1° towards the south. There was no apparent basement.

(a)

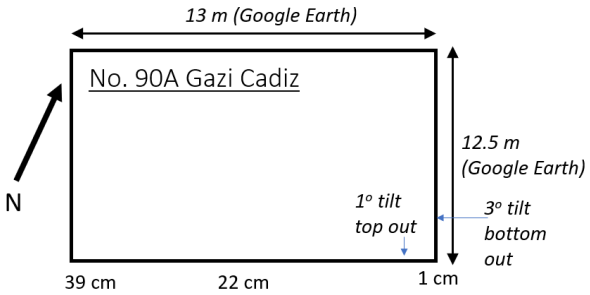

(b)

Figure 3.44. No. 90A Gazi Street (a) (37.7882N, 37.6437E; 30MAR2023) street view, and (b) schematic illustration of hand-surveyed settlements, tilts, and estimated dimensions.

(h. Gölbaşı) No. 92 Gazi Street

No. 92 Gazi Street (37.7881N, 37.6431E) is a 6-story residential apartment. These 6-stories include a sub-grade first level apartment. The estimated settlement at the southeast and southwest corners, the measured tilts, and estimated dimensions (measured from Google Earth) are summarized in Figure 3.45. The building settlement at the southeast corner was estimated as 31 cm and the building settlement at the southwest corner was estimated as 12 cm, indicating a differential settlement of about 19 cm. The measured tilt on the west side of the building was 1° towards the west. The measured tilt at the front (south side) of the building was 4.6° towards the north.

(a)

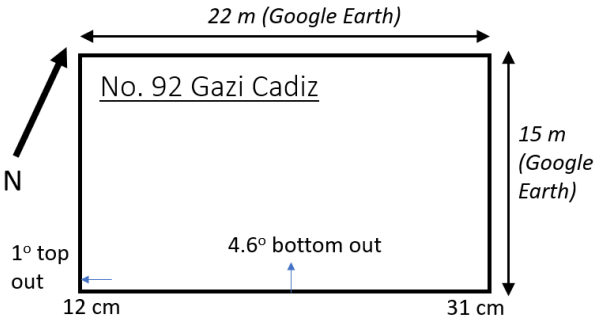

(b)

Figure 3.45. No. 92 Gazi Street (a) (37.7880N, 37.6432E; 30MAR2023) street view, and (b) schematic illustration of hand-surveyed settlements, tilts, and estimated dimensions.

(i. Gölbaşı) No. 94 Gazi Street

No. 94 Gazi Street (37.7880N, 37.6429E) is a 5-story building with no apparent basement (Figure 3.46a). The building appears to be residential. The estimated building settlement at the southwest corner was 11 cm and 51 cm at the southeast corner. The building tilt at the front (south) face was measured between 0 and 1.6° towards the south (top out). The estimated settlements, tilts, and dimensions are summarized in Figure 3.46b.

(a)

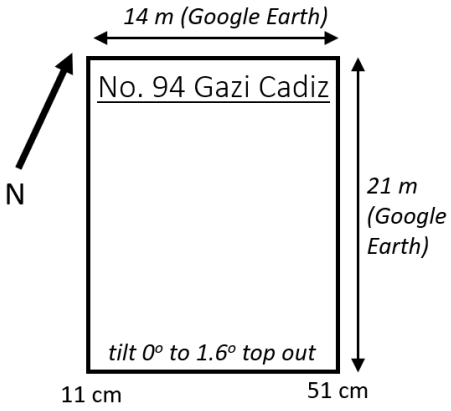

(b)

Figure 3.46. No. 94 Gazi Street (a) (37.7879N, 37.6429E; 30MAR2023) street view, and (b) schematic illustration of hand-surveyed settlements, tilts, and estimated dimensions.

4. TRANSPORTATION INFRASTRUCTURE

4.1 Bridges in Hatay Province

GEER Phase 3 team conducted detailed surveys of four damaged vehicular concrete bridges in the Antakya, Hatay Province region on March 31, 2023. The purpose of the GEER team visit was to observe and document geotechnical earthquake-induced damages, including zones of compression and extension along the bridge deck and superstructure, structural damage (e.g., cracks, spalling) at the bridge piers and pile caps, structural damages at the abutments, and soil and retaining wall failures near the abutments. Three of the bridges crossed the Orontes river and are labeled herein as the D817, Utku Acun Street, and Bekir Karabacak bridges, based on the supported highway or roadway. The fourth bridge crosses the Karasu river and is labeled herein as the Hatay Stadium bridge, due to its proximity to the stadium. Additional bridges that were fully functional were observed as well, however, they were not inspected in detail. All surveyed and observed bridges are mapped in Figure 4.1, along with the GPS track log of the GEER Phase 3 team. The map also indicates the locations of three nearby seismic recording stations: TK.3123, TK.3124, TK.3129, and TK.3132, which produced recorded ground accelerations that were among the most intense recorded during the 2023 Kahramanmaraş earthquake sequence.

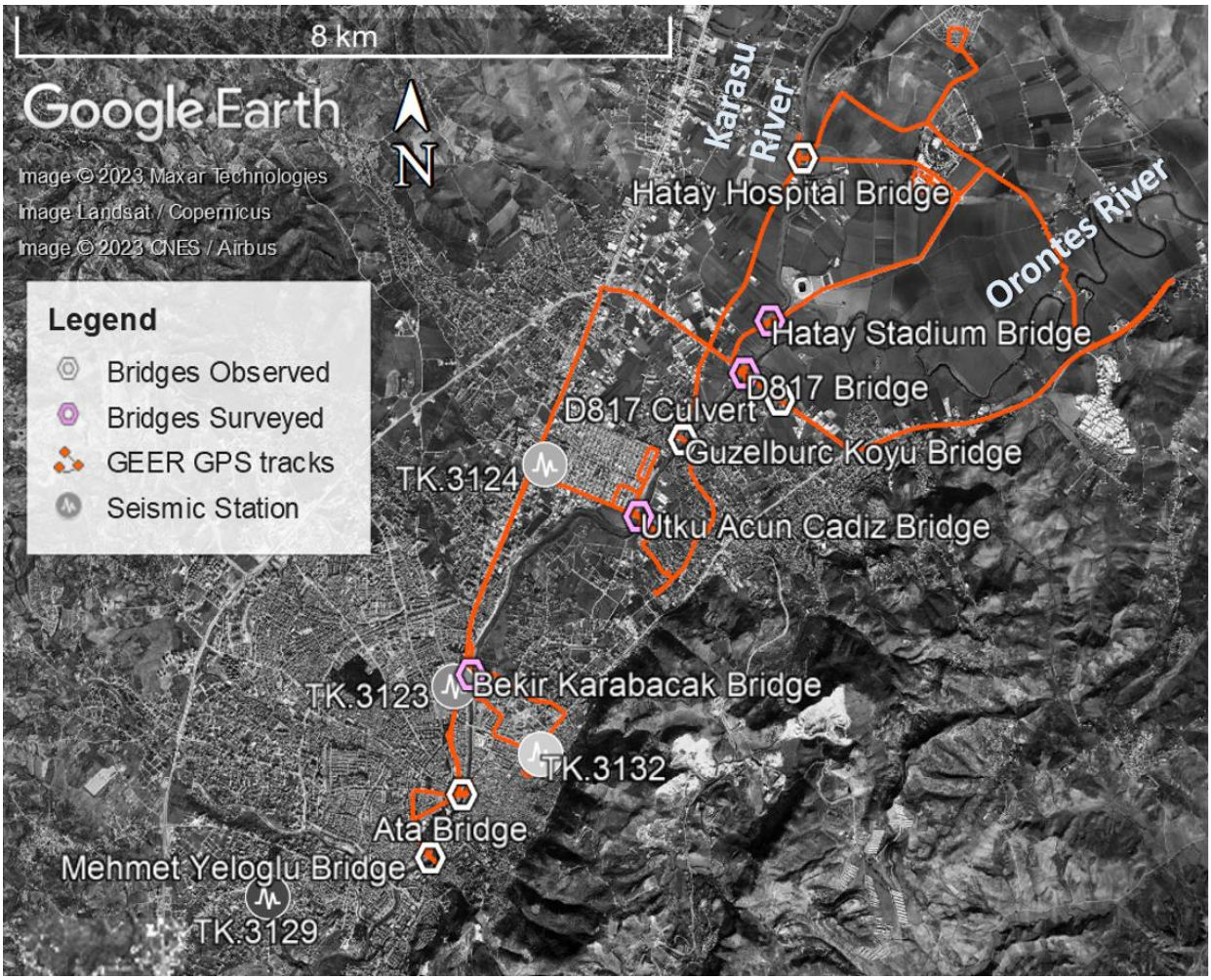

Figure 4.1. Map of observed bridges in Antakya, Hatay Province, Türkiye (Google Earth© 23DEC2022, centered near 36.2401N, 36.1882E).

4.1.1 D817 Bridge (36.2487N, 36.1998E)

The D817 Bridge crossing the Orontes river was open to traffic at the time of the GEER Phase 3 team investigation on March 31, 2022. Each 100 m long bridge structure of this twin bridge is supported on four hammerhead-shaped piers and two concrete abutments with underlying drilled shafts (four 70 cm diameter shafts per abutment). The 5-span twin bridge is located about 1.2 km southwest of the Hatay stadium, near agricultural areas north of the Antakya city center. It is located just southwest of the confluence of the Karasu river with the Orontes river, in a linear portion of the river that appears to have been channelized. A drone image of the twin bridge decks taken from the east bank of the Orontes river is shown in Figure 4.2. A post-earthquake satellite image of the bridge decks is shown in Figure 4.3 with some of the observations by the GEER team labeled. The aerial image, taken within 8 days after the earthquake, depicts recent road patches at all four bridge deck approaches and active traffic along the bridge decks.

The south and north bridge abutments along the east bank were visually inspected. Compression cracking and concrete spalling was observed at the south edge of the deck and abutment interface as shown in Figure 4.4a. The guardrails were detached in this area, such that the bridge deck may have shifted slightly north. This interface damage was possibly due to transitory structural pounding and grinding during the earthquake. One of the underlying abutment piles of the south bridge structure on the east bank was visible, where a roughly 0.5 cm tension crack was present about 15 cm from top of the pile. About a 1^{o} bottom-out tilt was measured at the abutment face on the south bridge structure (Figure 4.4b). The piles were not visible at the north abutment on the east bank; no tilt was measured at this abutment face.

Figure 4.2. Drone image of D817 Bridge crossing the Orontes River viewed from the east bank (36.2482N, 36.1999E; 31MAR2023).

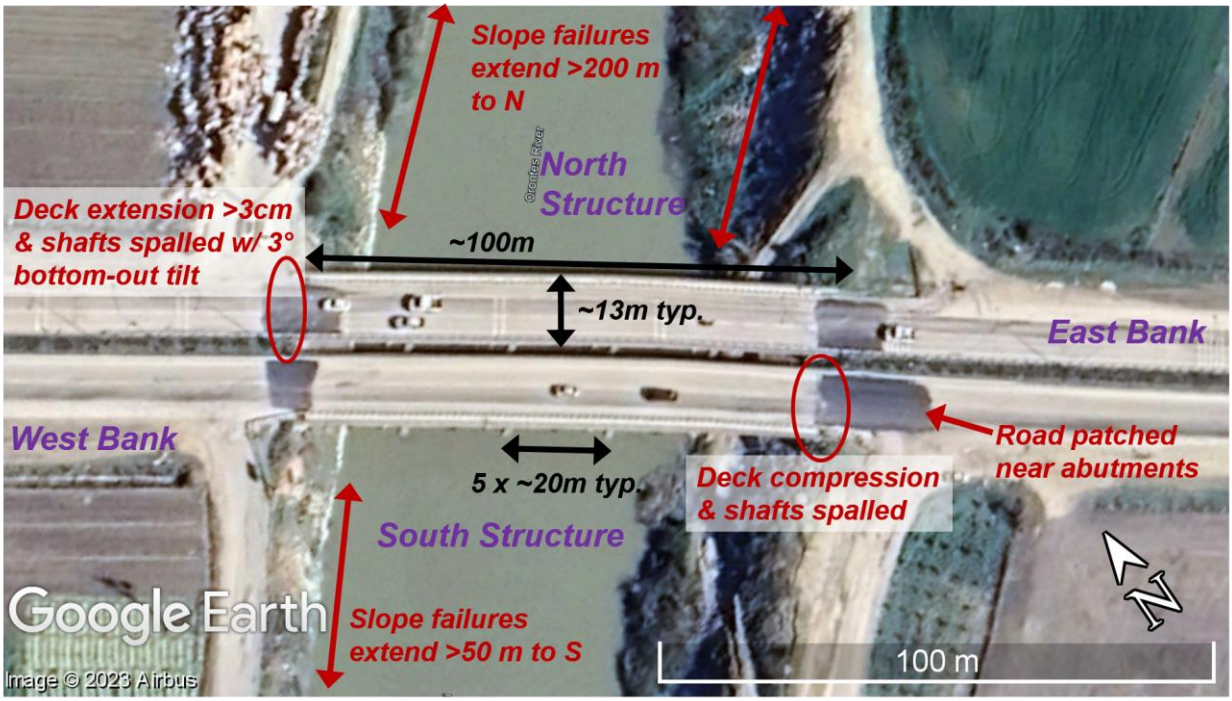

Figure 4.3. D817 Bridge detailed aerial map (Google Earth© Airbus, 14FEB2023).

The north and south bridge structure abutments along the west bank were also visually inspected. The north side of the north bridge structure abutment shown in Figure 4.5a, depicts a detached guardrail, a separated concrete deck block, and a 3 cm extensional opening at the top of the deck. The opening on the south side of the same bridge and abutment was observed to be more closed, although no measurements were recorded (Figure 4.5b). The conditions below the deck for the north bridge abutment are shown in Figure 4.5c. As seen at the left edge of this photo, the portion of the abutment beneath the bridge deck had a vertical hairline crack near its south edge, extending through the top half of its face. The abutment face was also measured beneath the bridge deck to have a bottom-out tilt of about 3º. A 3º dip of the deck surface was also measured above this area relative to the approach. The upper ~50 cm of three of the four underlying drilled shafts were exposed, showing visible concrete spalling and 0.5 to 1 cm thick horizontal tension cracks. Concrete spalling was similarly observed along the top of all four shafts for the south bridge abutment (e.g., Figure 4.5d). However, insignificant tilting (< 1º) was observed for this south bridge abutment.

Soil slumping failures and potentially rotational earth slides were observed along both the east and west banks near the D817 bridge. Movements were most significant near the crest of the banks located north of the bridges and appeared to extend 200 m north of the bridge. The movements were measured to spatially vary along the northwest bank with distance from the bridge deck. Within 20 m north of the bridges, a ground crack along the west bank had about 10 to 30 cm of vertical offset (Figure 4.6a), with horizontal offsets of a similar magnitude. About 70 m north of the bridge, in front of a warehouse facility, horizontal cracks of up to at least 80 cm wide were measured (Figure 4.6b). Movement was also observed along the west bank, south of the bridges,

as shown in Figure 4.6c. Lateral offsets of about 30 to 50 cm, and vertical offsets of about 50 to 60 cm were measured in this area. The slope movements along the river banks displayed ground movements that were consistent with the observed bottom-out tilt of the abutments which induced cracking in some of the piles.

(a) (b)

Figure 4.4. D817 Bridge damage at south bridge structure east bank abutment: (a) spalled concrete and movement at deck interface (36.2483N, 36.2001E; 31MAR2023), (b) abutment face (36.2485N, 36.2001E; 31MAR2023).

(a)

(b)

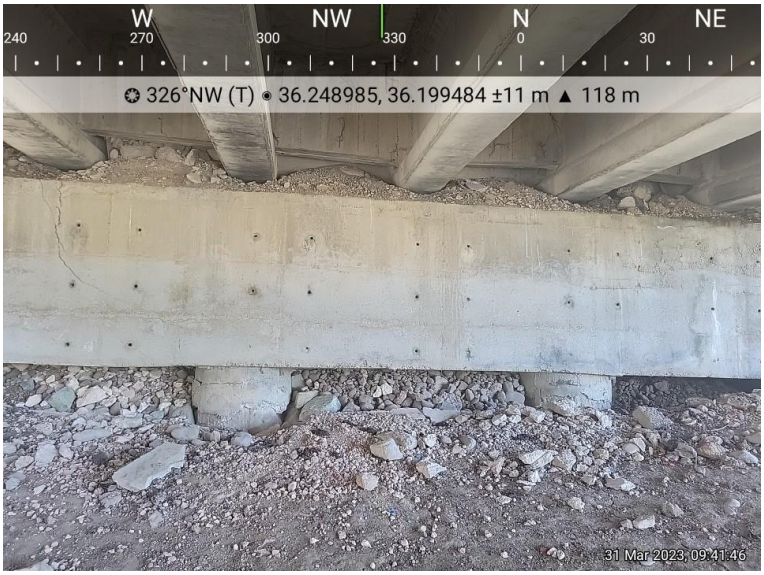

(c)

(d)

Figure 4.5. D817 Bridge damage at west bank abutments: (a) extensional cracks and deck tilt at north side of abutment interface with north bridge (36.2490N, 36.1994E; 31MAR2023), (b) slight separation at south side of abutment interface with north bridge (36.2490N, 36.1994E; 31MAR2023) (c) abutment face crack and spalling of drilled shafts at north bridge (36.2490N, 36.1995E; 31MAR2023), (d) spalling of drilled shaft at south bridge (36.2489N, 36.1993E; 31MAR2023).

(a)

(b)

(c)

Figure 4.6. Local slope failures along west bank near the D817 Bridge: (a) head scarp near north bridge with 10 to 30 cm vertical offset (36.2492N, 36.1995E; 31MAR2023) (b) head scarp north of bridges with up to 80 cm lateral offset and 10 to 30 cm vertical offset (36.2496N, 36.2000E; 31MAR2023), (c) head scarp south of bridges with 30 to 50 cm lateral offset and 50 to 60 cm vertical offset (36.2487N, 36.1990E; 31MAR2023).

4.1.2 Hatay Stadium Bridge (36.2545N, 36.2033E)

A twin bridge situated within 500 m of the Hatay Stadium, which crosses the Karasu river, was heavily damaged and closed to regular traffic at the time of the GEER Phase 3 team investigation on March 31, 2022. The 'Hatay Stadium' Bridge is located 200 m north of the confluence of the Karasu river with the Orontes river. The bridge decks are about 143 m long, with an 11 m wide

south bridge structure (Figure 4.7a) and a 16 m wide north bridge structure (Figure 4.7b). The south bridge is supported on four bents with two piers each and the north bridge is supported over four bents with three piers each, with large concrete abutments supporting the end spans of both bridges. A post-earthquake satellite image of the bridge decks is shown in Figure 4.8 with some of the observations by the GEER team labeled.

(a) (b)

Figure 4.7. 'Hatay Stadium' Bridge viewed from the east bank of the Karasu River: (a) south bridge structure (36.2547N, 36.2039E; 31MAR2023), and (b) north bridge structure (36.2550N, 36.2041E; 31MAR2023).

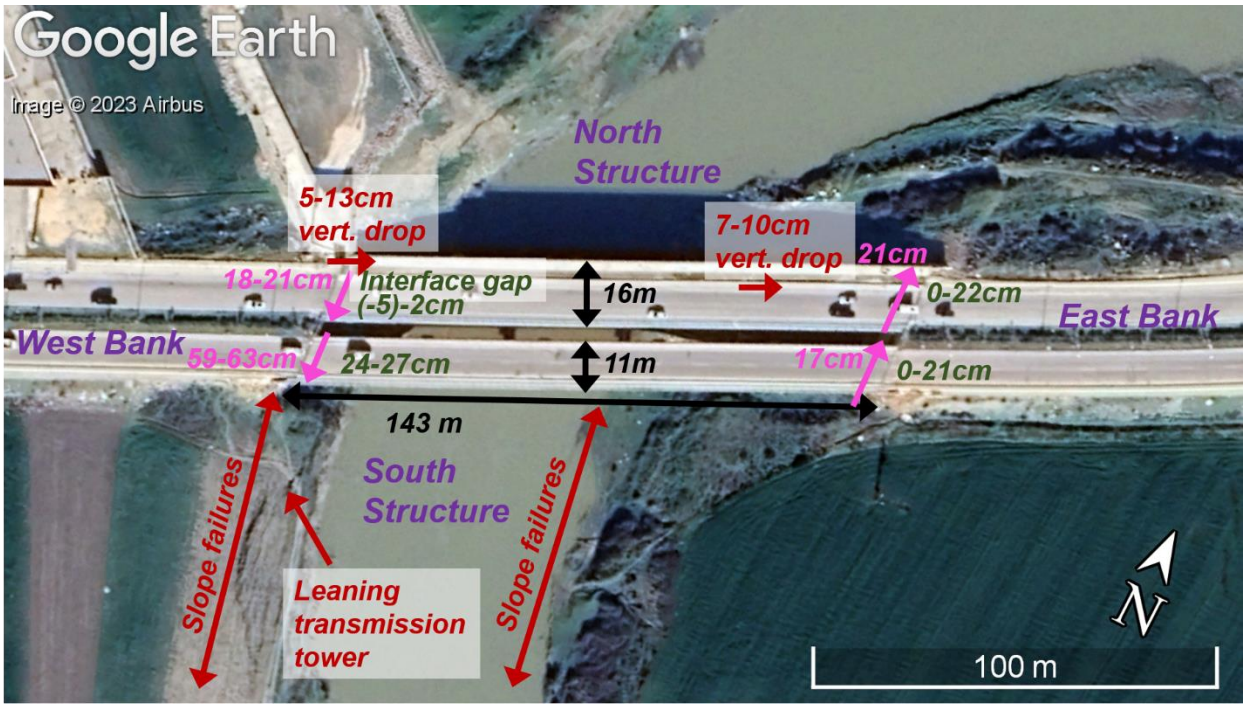

Figure 4.8. Hatay Stadium Bridge detailed aerial map (Google Earth© Airbus, 14FEB2023).

Significant damage was observed at the east abutment likely attributed to pounding and sliding of both bridge span decks against the abutment interface, as well as overall soil settlement and instability near the abutment. Cracking and spalling were observed at the edge of the north bridge deck and abutment (Figure 4.9a). The guardrail along the abutment approach had completely detached and fallen to the base of the abutment. Both bridge decks transversely displaced in a right-lateral direction by 21 cm at the north bridge and 17 cm at the south bridge along the east abutment interface (Figure 4.9b). Gaps at the deck-approach interface were measured to vary from 0 to 22 cm at the north bridge and 0 to 21 cm at the south bridge. The east approach had also settled relative to both bridge span decks, and some apparent roadway patching was present along the interface, likely to allow vehicle access after the earthquake (Figure 4.9c).

(a) (b) (c)

Figure 4.9. Damage at east abutment of Hatay Stadium Bridge: (a) cracking and spalling at edge of north bridge deck and abutment (36.2551N, 36.2041E; 31MAR2023), (b) right-lateral offset at edge of north bridge deck (36.2550N, 36.2042E; 31MAR2023), (c) settlement of abutment and misalignment of deck at south bridge (36.2548N, 36.2043E; 31MAR2023).

The easternmost bents of both bridges were visually inspected. The shear keys at the pier cap were severely damaged, and spalling was observed at the base of the columns (Figure 4.10a). However, the concrete foundations of the bents appeared to be stable and unmoved (Figure 4.10b). It is not known if slope-induced ground movements may have affected foundation performance. Ground shaking was intense in this area, so much of the observed damage could have been caused by the intense transient ground motions produced by the earthquakes. A 7-10 cm vertical drop was measured with a laser level along the south bridge deck from west to east across the bent (Figure 4.10c).

(a)

(b)

(c)

Figure 4.10. Damage at eastern-most bent of Hatay Stadium Bridge: (a) damage of shear keys at pier cap and base of columns (36.2551N, 36.2041E; 31MAR2023), (b) pile caps are undamaged (36.2549N, 36.2040E; 31MAR2023), and (c) vertical drop of deck measured by laser level across cracks observed above the bent (36.2548N, 36.2037E; 31MAR2023).

Significant damage was additionally observed at the west abutment. The reinforced concrete girders of the south bridge exhibited cracks and spalling (Figure 4.11a, 4.11b). The girders had translated by 59 to 63 cm to the south, as measured from the deck surface. The north bridge of the twin bridge had also translated by 18 to 21 cm to the south, relative to the west approach. Gaps at the deck-approach interface were measured to vary from 24 to 27 cm at the south bridge, and -5 (i.e., compression observed as pavement overlap) to 2 cm at the north bridge. The approach was 5 to 13 cm above the north span deck.

(a)

(b)

Figure 4.11. Damage at west abutment of Hatay Stadium Bridge: (a) south bridge girder damage (36.2542N, 36.2028E; 31MAR2023), and (b) settlement and misalignment of deck at north end of abutment (36.2542N, 36.2028E; 31MAR2023).

Soil slump failures and potentially rotational earth slides of the underlying and surrounding soil slopes were observed. Slope failures were observed under the west end of the bridge, within earth

in front of the west abutment. A scarp with a vertical offset of about 1 m was located 3 to 5 m from the westernmost bents (Figure 4.12a). However, contrary to expectations of a rotational failure, the westernmost bents (south bridge) were measured to tilt forward towards the river by about 1°. A transmission tower, located 20 m south of the west abutment near the scarp of a larger ground movement, was observed to have a strong river-oriented lean (Figure 4.12b).

(a)

(b)

Figure 4.12. Local slope failures near Hatay Stadium Bridge: (a) rotational sliding beneath west end of bridge (36.2542N, 36.2029E; 31MAR2023), and (b) lateral spreading along east bank (background) and rotational failure affecting transmission lines on west bank (foreground) of Karasu river (36.2540N, 36.2029E; 31MAR2023).

4.1.3 Bekir Karabacak Bridge (36.2155N, 36.1621E)

Only the north bridge structure of the twin-parallel Bekir Karabacak Bridge structures, each with 3 spans that cross the Orontes River in Antakya, was open to traffic at the time of the GEER Team 3 investigation on March 31, 2022. Each 48-m long and 14-m wide bridge structure is supported with two concrete wall piers and two concrete wall abutments. The twin bridge is located within a densely populated area of the city. Both banks of the Orontes river are lined with a concrete facing in this area. The twin bridge abutments are connected to soil retaining wingwalls that taper towards and adjoin the riverbank facings. The wingwalls at all four corners of the twin bridge had failed following the earthquakes. An image of the bridge taken from the west bank of the river, near is shown in Figure 4.13. A post-earthquake satellite image of the twin bridge is shown in Figure 4.14 with some labeled observations.

Significant displacements and damage were observed along the deck of the south bridge structure. At the east end of the bridge, the deck was uplifted by 37 cm relative to the adjacent approach (Figure 4.15a). At the west end of the bridge, significant compressive deformations were apparent from amid broken up and compressed pavement slabs. Measurements of the displaced pavement slabs atop the bridge decks slabs suggest that the deck had compressed towards the approach with a displacement of about 50 cm at the south end and 20 cm at the north end of the south span (Figure 4.15b). A thin mound of soil was also observed across the deformations in this area, likely to allow easier access for construction traffic. Above and parallel to the wall piers, the bridge deck

sustained extensional cracks as depicted in Figure 4.15c. A pipeline along the south span deck appeared to have generally compressed (Figure 4.15d).

Figure 4.13. The Bekir Karabacak Bridge crossing the Orontes River, as viewed from near a retaining wall failure at the northwest wingwall of the bridge (36.2160N, 36.1619E; 31MAR2023).

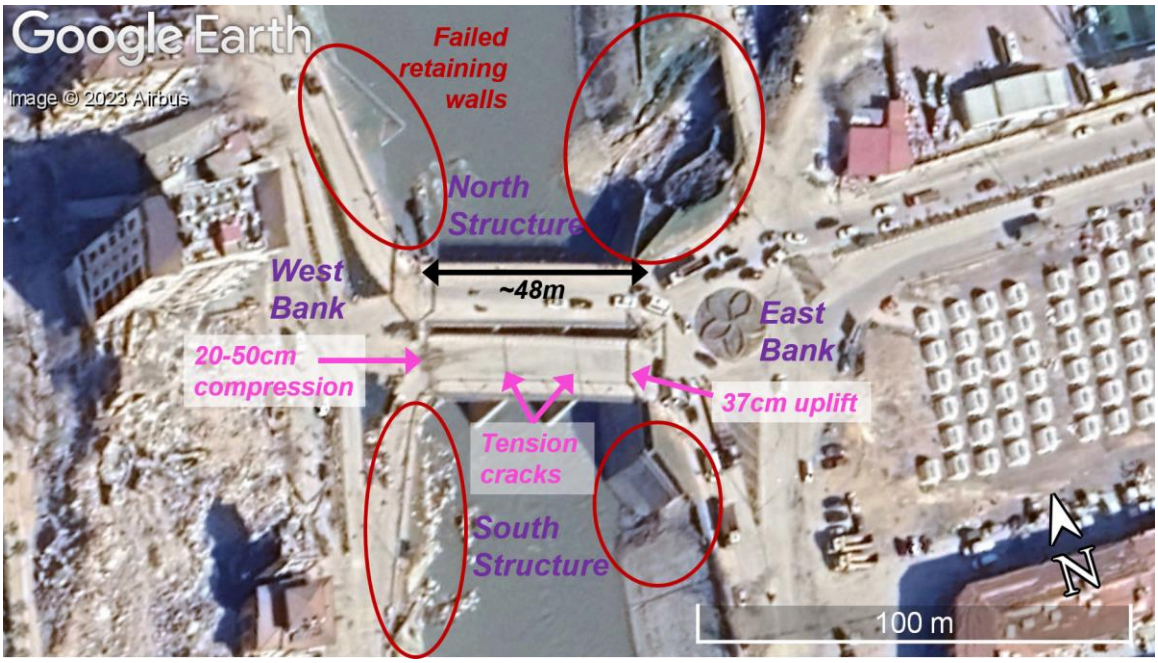

Figure 4.14. Bekir Karabacak Bridge detailed aerial map (Google Earth© Airbus, 14FEB2023)

(a) (b)

(c) (d)

Figure 4.15. Deformations along south bridge deck: (a) east edge of deck is 37 cm higher than adjacent approach (36.2153N, 36.1624E; 31MAR2023), (b) pavement buckling with up to 50 cm of compression (36.2156N, 36.1619E; 31MAR2023), (c) extensional cracks above wall piers (36.2154N, 36.1620E; 31MAR2023), (d) observed compression along pipeline (36.2153N, 36.1624E; 31MAR2023).

Retaining wall failures were observed at the wingwalls of all four corners of the Bekir Karabacak twin bridge. The failures at the northwest and northeast corners of the bridges are depicted in Figure 4.16a, and failures at the southwest and southeast corners are depicted in Figure 4.16b. The overall wall height above the water is over 6 m based on a rough estimate. The failures along the west bank revealed the retained fill as containing a significant volume of large cobbles and boulders. The east bank fills contained smaller cobbles and rock fragments, and was primarily composed of finer soils. It appeared that the bridge decks helped to restrain partially the movement of the abutment walls.

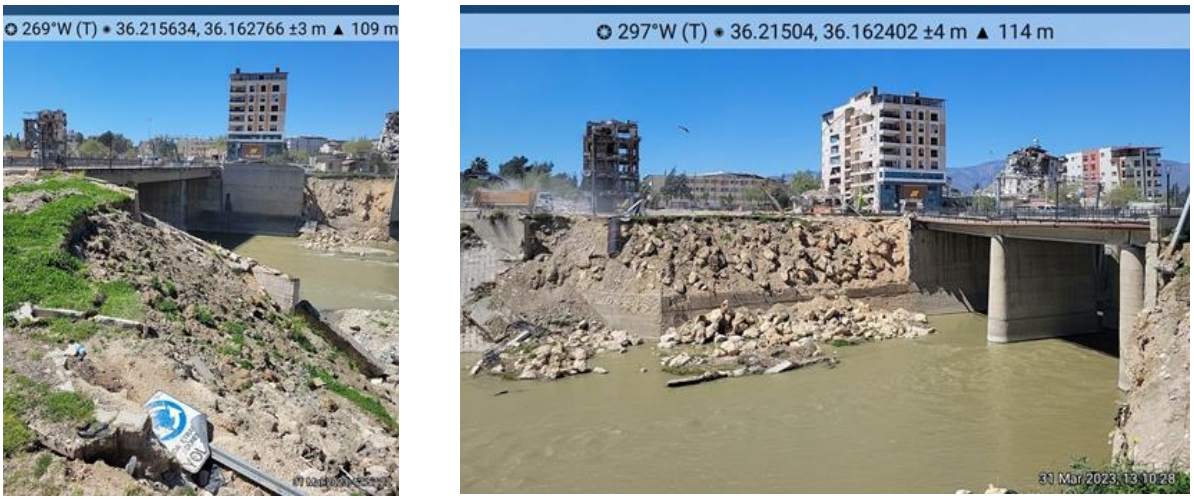

(a) (b)

Figure 4.16. Retaining wall failures: (a) northeast failure in foreground and northwest failure in background (36.2156N, 36.1628E; 31MAR2023), and (b) southwest failure in background and partial view of southeast failure in foreground (36.2150N, 36.1624E; 31MAR2023).

4.1.4 Utku Acun Street Bridge (36.2329N, 36.1852E)

The Utku Acun Street Bridge crossing the Orontes River was open to regular traffic at the time of the GEER Phase 3 team investigation on March 31, 2022. Each 117-m long and 11-m wide bridge of this twin-parallel 3-span bridge structure is supported with two cap and dual-column piers and two concrete abutments. In addition to carrying two lanes of traffic, the south bridge structure also supports a gas or water pipeline that appears to have remained serviceable. The twin bridge is situated near a meander of the Orontes river, north of the Antakya city center. An image of the twin bridge taken from the east bank of the Orontes river is shown in Figure 4.17. A post-earthquake satellite image of the bridges is shown in Figure 4.18 with some labeled observations.

Figure 4.17. The Utku Acun Street Bridge crossing the Orontes River, as viewed from the east bank, south of the twin bridge (36.2326N, 36.1855E; 31MAR2023).

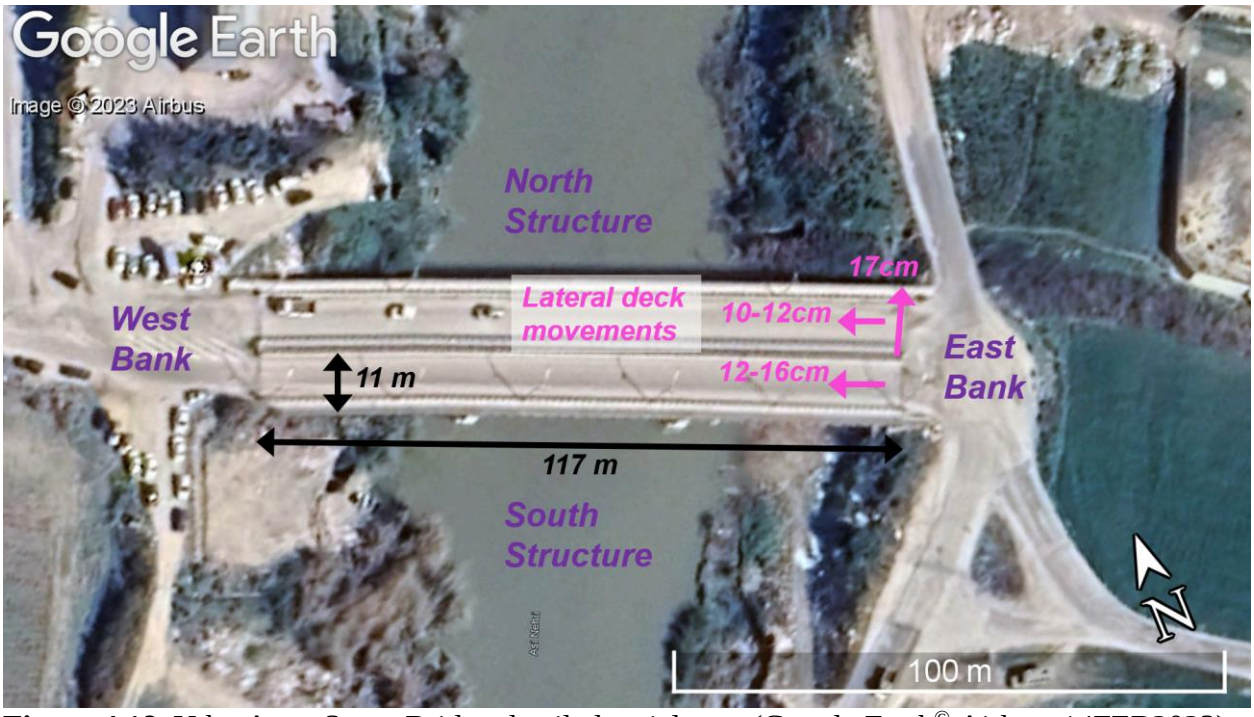

Figure 4.18. Utku Acun Street Bridge detailed aerial map (Google Earth© Airbus, 14FEB2023).

The east abutment was inspected in greatest detail, due to ease of accessibility and more obvious damage. The portion of the abutment supporting the north and south bridge deck approaches was damaged with compressive fractures and spalling near the base of the deck girders. The bridge approach sections were tilted down away from the river at an angle of 1 to 2º. This resulted in a gap of 10-12 cm at the north bridge (Figure 4.19a), and 12-16 cm at the south bridge, as measured along the approach-to-deck interface at the road surface. The north bridge structure deck shifted right laterally (northward) by 17 cm (Figure 4.19b), whereas such transverse movements were not apparent for the south bridge structure deck and supporting pipeline. Below the deck, the girders were cracked, and shear key damage between the girders was observed. The girders had clearly shifted relative to the bearing pads beneath them.

The soil in front of the east abutment exhibited several extensional cracks as observed in Figure 4.20 due to ground movements towards the river channel. Soil along both the east and west banks adjacent to the bridge were heavily vegetated during our investigation, but appeared to show similar lateral movements towards the river. Pre- and post-earthquake Google Earth satellite imagery also suggests a constricting of the river channel due to translational movements of the banks, within about 500 m of this bridge. Movements are most apparent along the river meander to the south.

(a)

(b)

(c)

Figure 4.19. Damage at east abutment of Utku Acun Street Bridge: (a) north side of abutment is tilted 1° to 2° back (deck approach shifted away from river), with a separation gap of over 12 cm near the deck (36.2329N, 36.1858E; 31MAR2023), (b) north bridge deck shifted about 17 cm to the north (36.2329N, 36.1858E; 31MAR2023), and (c) girder and shear key damage (36.2327N, 36.1856E; 31MAR2023).

Figure 4.20. Ground cracks below the east bridge span in front of the east abutment indicated lateral movement toward the river (36.2327N, 36.1856E; 31MAR2023).

4.1.5 Other Observed Bridges

Several other bridges and a culvert in Antakya were briefly observed by the GEER team and judged to be in a functional state. These included the 'Hatay Hospital' bridge (36.2726N, 36.2078E), Guzelburc Koyu (36.2413N, 36.1913E), Ata (36.2023N, 36.1609E), and Mehmet Yeloglu bridges (36.1953N, 36.1565E), as well as the D817 culvert (36.2457N, 36.2047E).

The main bridge near the Hatay Egitim ve Arastirma Hastanesi (hospital) crossing the Karasu river was open to traffic and appeared to not be damaged during a brief drive-by observation. However, local soil slumping failures were observed along the east bank adjacent to the bridge (Figure 4.21). The three easternmost deck spans of an old bridge just south of the main bridge collapsed.

Figure 4.21. Local slumping failure and collapse of old bridge deck along east bank to the south (background of photo) of the main 'Hatay Hospital' Bridge (foreground of photo) (36.2456N, 36.2047E; 31MAR2023).

A culvert beneath the D817 highway, near the D817 bridge, was briefly observed (Figure 4.22). The roadway above the culvert appeared to be recently patched. The concrete retaining wall adjacent to the culvert was displaced towards the channel by at least half a meter.

Figure 4.22. Retaining wall damage near a culvert beneath the D817 highway (36.2726N 36.2083E; 31MAR2023).

4.2 Underpass in İskenderun, Hatay

Post-earthquake flooding was observed in the D817 underpass (located in İskenderun, Hatay) on Google Earth images from February 8, 2023 (Figure 4.23). The underpass is approximately 7.5 m deep (measured with a laser distance tool) from the surface of the road-level at the intersection of İsmet İnönü Street and D817 (36.5829N, 36.1690E). The GEER Phase 3 team observed negligible damage (i.e., absence of tilting or cracking in retaining walls, deformation or cracks in road pavement) to the underpass structure on March 28, 2023 (Figure 4.24a). Some damage to the surface road-level sidewalks was observed (Figure 4.24b). Local taxicab drivers reported that the underpass flooded with about 1 m of water and a significant amount of sand soon after the earthquakes. The approximate elevation of the surface road at the İsmet İnönü Street and D817 intersection is 10.5 m to 11 m above sea level (GPS elevation), which indicates the elevation of the underpass roadways is approximately 2.5 m to 3 m above sea level at this location. On March 28, 2023 some seepage was observed at the retaining wall joints and storm drains (Figure 4.24c). The GEER Phase 3 team observed no flooding in the underpass on March 29 when major flooding occurred in the shorefront areas of İskenderun.

Figure 4.23. Image of u-box underpass in İskenderun, Hatay from Google Earth on February 8, 2023, showing flood water in the underpass. Center of the image is approximately 36.5832N, 36.1697E.

(a) (b) (c)

Figure 4.24. U-box underpass in İskenderun, Hatay: (a) (36.5829N, 36.1691E; 28MAR2023) negligible damage observed along retaining wall, (b) (36.5828N, 36.1679E; 28MAR2023) sidewalk damage from the street level above the underpass, and (c) (36.5825N, 36.1678E; 28MAR2023) drainage from storm drains.

5. SUMMARY

The GEER Phase 3 team reconnaissance focused on geotechnical effects from the February 6 Kahramanmaraş earthquake sequence. Reconnaissance included the survey of liquefaction and lateral spread effects in İskenderun and Gölbaşı. The observations included lateral spreading, ground settlement, and frequent flooding that appears related to the earthquakes. The effects of liquefaction on buildings were also surveyed, including measurements of settlement, tilting, and ground-building interactions. Measurements were performed with hand-surveys with laser levels and terrestrial lidar scan data. Reconnaissance was also performed in the city of Antakya. No evidence of liquefaction was observed within Antakya. The performance of some vehicular concrete bridges was surveyed in and around Antakya. While several bridges remained functional after the earthquakes, significant structural damages were observed at the bridge superstructures, piers, abutments, and surrounding riverbank slopes and retaining walls.

The documentation of the building settlement case histories requires follow-on studies to characterize the subsurface conditions at key sites to add these case histories to the limited number of existing well documented case histories of building performance during major earthquakes. Learning from the effects of the lateral spreading cases also requires subsurface characterization. Additionally, the subsurface characteristics at sites with relatively high PI ejecta should be investigated. Lastly, the effects of flooding following an earthquake should be studied further.

6. ACKNOWLEDGEMENTS

The work of the GEER Association is supported in part by the National Science Foundation through the Engineering for Civil Infrastructure Program under Grant No. CMMI1826118. Any opinions, findings, and conclusions or recommendations expressed in this material are those of the authors and do not necessarily reflect the views of the NSF. Any use of trade, firm, or product names is for descriptive purposes only and does not imply endorsement by the U.S. Government. The GEER Association is made possible by the vision and support of the NSF Geotechnical Engineering Program Directors: Dr. Giovanna Biscontin, Dr. Richard Fragaszy, and the late Dr. Cliff Astill. GEER members also donate their time, talent, and resources to collect time-sensitive field observations of the effects of extreme events. Researchers from the Middle East Technical University received support from the Turkish government. Additionally, Zemin Etüd vs Tasarim A.Ş. provided financial support for a team member, and Dr. H. Turan Durgunoğlu provided guidance and logistical support to the team. Dr. Adam Booth (Portland State University) provided the lidar equipment, as well as training on the equipment and data analysis. The team is also grateful to the knowledge and support provided by Dr. Murat Bikçe (İskenderun Technical University), Dr. Halil Sezen (The Ohio State University), and Ezra Jampole (Exponent).

7. REFERENCES

GEER-EERI (2023). February 6, 2023 Türkiye Earthquakes: Report on Geoscience and Engineering Impacts. GEER Association Report 082. https://10.18118/G6PM34. May 6, 2023.

Ishihara, K., Yasuda, S., and Nagase, H. (1996). "Soil characteristics and ground damage." Special Issue on Geotech. Aspets of the Jan 17 1995 Hyogoken-Nambu Earthquake." Soils and Foundations, JGS, Jan., 109-118.

Nalça, C. (2018). "Transformation of İskenderun Historic Urban Fabric from Mid 19th Century to the end of the French Mandate Period." Masters Thesis, Izmir Institute of Technology, Graduate School of Engineering and Sciences.

Okuwaki, R., Yagi, Y., Taymaz, T., and Hicks, S. (2023). "Multi-Scale Rupture Growth with Alternating Directions in a Complex Fault Network During the 2023 South-Eastern Türkiye and Syria Earthquake Doublet." Geophysical Research Letters. 10.1029/2023GL103480.

Papageorgiou, E., Foumelis, M & Delgado Blasco, J.M. (2023). Pre-seismic Sentinel-1 PSI surface motion measurements for the area affected by the February 2023 Türkiye–Syria earthquakes (1.0) [Data set]. Zenodo. https://doi.org/10.5281/zenodo.7672169

Pease, J. W., & O'Rourke, T. D. (1997). "Seismic Response of Liquefaction Sites." Journal of Geotechnical and Geoenvironmental Engineering, 123(1), 37–45. https://doi.org/10.1061/(asce)1090-0241(1997)123:1(37).

Pradel, D., Wartman, J., & Tiwari, B. 2014. "Impact of Anthropogenic Changes on Liquefaction along the Tone River during the 2011 Tohoku Earthquake." Natural Hazards Review, ASCE, 15 (1). 10.1061/(ASCE)NH.1527-6996.0000097.

Robinson, K., Cubrinovski, M., Kailey, P., Orense, R. (2010). "Field Measurements of Lateral Spreading following the 2010 Darfield Earthquake." Proc., Ninth Pacific Conference on Earthquake Engineering Building an Earthquake-Resilient Society, Auckland, New Zealand.

Taftsoglou Maria, Valkaniotis Sotiris, Karantanellis Efstratios, Goula Evmorfia, & Papathanassiou. (2023). "Preliminary mapping of liquefaction phenomena triggered by the February 6 2023 M7.7 earthquake, Türkiye / Syria, based on remote sensing data." Zenodo. https://doi.org/10.5281/zenodo.7668401

Uggeri, G. (1998). "L'urbanistica di Antiochia sull'Oronte," Journal of Ancient Topography 8: 179-222.

United States Geological Survey. (2023, June 30). *The 2023 Kahramanmaras, Turkey, Earthquake Sequence*. https://earthquake.usgs.gov/storymap/index-turkey2023.html